

การเตรียมอนุภาคพอลิ(นอร์มัลบิวทิลแอสไตรเลต-โค-เมทิลเมทาคริเลต)ที่ห่อหุ้มด้วยไคโตซาน

นางสาววิกานดา ทวีรัตน์

วิทยานิพนธ์นี้เป็นส่วนหนึ่งของการศึกษาตามหลักสูตรปริญญาวิทยาศาสตรมหาบัณฑิต

สาขาวิชาปิโตรเคมีและวิทยาศาสตร์พอลิเมอร์

คณะวิทยาศาสตร์ จุฬาลงกรณ์มหาวิทยาลัย

ปีการศึกษา 2551

ลิขสิทธิ์ของจุฬาลงกรณ์มหาวิทยาลัย

**PREPARATION OF POLY(*n*-BUTYL ACRYLATE-*co*-METHYL  
METHACRYLATE) PARTICLES ENCAPSULATED WITH CHITOSAN**

**Miss Wikanda Taweerat**

**A Thesis Submitted in Partial Fulfillment of the Requirements for the Degree of**

**Master of Science Program in Petrochemistry and Polymer Science**

**Faculty of Science**

**Chulalongkorn University**

**Academic year 2008**

**Copyright of Chulalongkorn University**

Thesis Title            PREPARATION OF POLY(*n*-BUTYL ACRYLATE-*co*-  
METHYL METHACRYLATE) PARTICLES  
ENCAPSULATED WITH CHITOSAN

By                         Miss Wikanda Taweerat

Field of Study         Petrochemistry and Polymer Science

Advisor                 Siriwan Phattandarudee, Ph.D.

---

Accepted by the Faculty of Science, Chulalongkorn University in Partial  
Fulfillment of the Requirements for the Master's Degree

..... Dean of the Faculty of Science  
(Professor Supot Hannongbua, Dr.rer.nat.)

THESIS COMMITTEE

..... Chairman  
(Professor Pattarapan Prasassarakich, Ph.D.)

..... Advisor  
(Siriwan Phattandarudee, Ph.D.)

..... Examiner  
(Assistant Professor Warinthorn Chavasiri, Ph.D.)

..... External Examiner  
(Wiyong Kangwansupamonkon, Ph.D.)

วิกานดา ทวีรัตน์ : การเตรียมอนุภาคพอลิ(นอร์มัลบิวทิลแอคริเลต-โค-เมทิลเมทาคริเลต)ที่ห่อหุ้มด้วยไคโตซาน (PREPARATION OF POLY(*n*-BUTYL ACRYLATE-*co*-METHYL METHACRYLATE) PARTICLES ENCAPSULATED WITH CHITOSAN อ.ที่ปรึกษาวิทยานิพนธ์หลัก : อ. ดร. สิริวรรณ พัฒนาฤดี, 79 หน้า

งานวิจัยนี้ศึกษาการเตรียมอิมัลชันของโคพอลิเมอร์ที่ประกอบด้วยมอนอเมอร์ที่มีลักษณะอ่อนนุ่มและมีลักษณะแข็ง ได้แก่ นอร์มัล-บิวทิลแอคริเลต (*n*-butyl acrylate, *n*-BA) และเมทิลเมทาคริเลต (methyl methacrylate, MMA) ตามลำดับ โดยผสมที่อัตราส่วนแตกต่างกัน และห่อหุ้มด้วยไคโตซานที่มีความเข้มข้นร้อยละ 0.5-1.5 โดยน้ำหนัก ซึ่งไคโตซานที่ใช้มีน้ำหนักโมเลกุล  $1.2 \times 10^5$  Da,  $3.7 \times 10^5$  Da, และ  $8.5 \times 10^5$  Da โดยมีร้อยละของการกำจัดหมู่แอซิดิล 87-88% และศึกษาสมบัติเชิงคอลลอยด์และลักษณะของฟิล์ม พบว่าเปอร์เซ็นต์ผลผลิตของโคพอลิเมอร์มีค่าค่อนข้างสูง (ประมาณ 80-90%) ลักษณะของอนุภาคด้วยเทคนิค TEM ซึ่งแสดงภาพถ่ายของอนุภาคพอลิ(นอร์มัลบิวทิลแอคริเลต-โค-เมทิลเมทาคริเลต)ที่ห่อหุ้มด้วยไคโตซาน พบอนุภาคมีลักษณะกลม ไคโตซานสามารถห่อหุ้มอนุภาคโคพอลิเมอร์ได้ดีเมื่อความเข้มข้นและน้ำหนักโมเลกุลของไคโตซานเพิ่มขึ้น และในอัตราส่วนที่มีนอร์มัลบิวทิลแอคริเลตปริมาณมากจะส่งผลให้ไคโตซานห่อหุ้มอนุภาคโคพอลิเมอร์ได้ดี ผลการวิเคราะห์ขนาดอนุภาคและประจุบนพื้นผิว พบว่าขนาดอนุภาคจะเพิ่มขึ้นตามปริมาณของไคโตซานและน้ำหนักโมเลกุล ประจุบนพื้นผิวมีค่าเป็นบวกซึ่งได้รับการโปรโตเนทจากไคโตซาน ผลการวัดความหนืดและแรงตึงผิวของลาเท็กซ์พบว่ามีค่าเพิ่มขึ้นเมื่อความเข้มข้นและน้ำหนักโมเลกุลของไคโตซานเพิ่มขึ้น โครงสร้างทางเคมีของอนุภาคโคพอลิเมอร์ที่ห่อหุ้มด้วยไคโตซานสามารถแสดงผลการวิเคราะห์ด้วยเทคนิค  $^1\text{H-NMR}$  โดย % grafting ขึ้นอยู่กับปริมาณของความเข้มข้นและน้ำหนักโมเลกุลของไคโตซาน ผลการตัดโค้งแผ่นฟิล์มพบว่าเมื่อปริมาณนอร์มัลบิวทิลแอคริเลตเพิ่มขึ้นแผ่นฟิล์มมีความยืดหยุ่นได้ดี ผลการวิเคราะห์ด้วยเทคนิค AFM พบลักษณะการเกิดแผ่นฟิล์มที่เรียบขึ้นเมื่อความเข้มข้นของไคโตซานเพิ่มขึ้นและความเรียบของแผ่นฟิล์มมีค่าเพิ่มขึ้นเมื่อปริมาณของนอร์มัลบิวทิลแอคริเลตเพิ่มขึ้น

สาขาวิชา..ปิโตรเคมีและวิทยาศาสตร์พอลิเมอร์..ลายมือชื่อนิสิต.....  
ปีการศึกษา.....2551..... ลายมือชื่ออ.ที่ปรึกษาวิทยานิพนธ์หลัก.....

## 4972481023 : MAJOR PETROCHEMISTRY AND POLYMER SCIENCE

KEY WORD : *n*-BUTYL ACRYLATE / METHYL METHACRYLATE / CHITOSAN

WIKANDA Taweerat : PREPARATION OF POLY(*n*-BUTYL  
ACRYLATE-*co*-METHYL METHACRYLATE) PARTICLES

ENCAPSULATED WITH CHITOSAN. ADVISOR : SIRIWAN

PHATTANARUDEE, Ph.D., 79 PP.

This research studied the preparation of copolymers containing soft and hard monomers, *n*-butyl acrylate (*n*-BA) and methyl methacrylate (MMA), respectively. The effect of monomer ratio, molecular weight, and concentration of chitosan on colloidal and film properties of the copolymer particles was investigated. The result showed that the percentage of monomer conversion was achieved at high conversion (approximately 85-90%). TEM micrographs of the copolymer particles and the copolymer particles encapsulated with chitosan showed that the particles obtained were spherical. The chitosan layer seemed to gain more thickness according to the molecular weight and concentration of chitosan. Measurements of particles size and surface charge of the copolymer encapsulated with chitosan indicated that the large size of particles were formed and positive charge was present on the particle surface when the chitosan was added. The chemical structure of the copolymer particles encapsulated with chitosan was characterized by <sup>1</sup>H-NMR in which % grafting of copolymers depended on the concentration and molecular weights of chitosan. The viscosity and surface tension of the encapsulated particles were increased when the chitosan content was increased from 0.5-1.5 %w/v. As the chitosan concentration was increased, the AFM micrographs exhibited that the roughness of copolymers was decreased. The result of bending test revealed the flexibility of the coating obtained from the encapsulated particles.

Field of Study : ..Petrochemistry and polymer science..Student's Signature.....

Academic Year : .....2008.....Advisor's Signature.....

## ACKNOWLEDGEMENTS

I would like to express the grateful appreciation to my advisor, Dr. Siriwan Phattanarudee, for providing valuable advice, encouragement, and assistance throughout the course of this research. Her review on the content of the thesis is extremely valuable and it is my heart felt gratitude to acknowledge her help. In addition, the author also wishes to express her deep appreciation to Dr. Pattarapan Prasassarakich, for serving as the chairman, Assistant Professor Dr. Warinthorn Chavasiri, for examiner, and Dr. Wiyong Kangwansupamonkon for external examiner of my thesis committee, for their valuable suggestion and comment.

Appreciation is also extended to the Program of Petrochemistry and Polymer Science, the Department of Imaging and Printing Technology in the Faculty of Science, Chulalongkorn University and National Center of Excellence for Petroleum, Petrochemicals and Advanced Materials (NCE-PPAM) for providing facilities.

Further acknowledgement is extended to my friends, especially Mr. Ekawit Laohataiwanich for his help, moral support, suggestion, and encouragement. Finally, I appreciate highly my family for their support, understanding and patience during the course of my study.

## CONTENTS

	Page
ABSTRACT IN THAI.....	v
ABSTRACT IN ENGLISH.....	vi
ACKNOWLEDGEMENTS.....	vii
LIST OF TABLE.....	xi
LIST OF FIGURE.....	xii
CHAPTER I INTRODUCTION.....	1
1.1 Scientific rational.....	1
1.2 Objectives.....	2
1.3 Scope and work plan.....	2
1.4 Expected benefit.....	2
CHAPTER II THEORY AND LITERATURE REVIEW.....	3
2.1 Emulsion polymerization.....	3
2.1.1 Ingredient in recipe.....	4
2.1.2 Monomers.....	4
2.1.3 Initiators.....	5
2.1.4 Surfactants.....	5
2.2 Core-shell morphologies.....	6
2.3 Chitin.....	7
2.4 Chitosan.....	7
2.5 Binder.....	9
2.6 Literature reviews.....	9

	Page
CHAPTER III EXPERIMENTS.....	13
3.1 Chemicals.....	13
3.1.1 <i>n</i> -Butyl acrylate ( <i>n</i> -BA).....	13
3.1.2 Methyl methacrylate (MMA).....	13
3.1.3 Chitosan.....	14
3.1.4 Potassium persulphate (KPS).....	14
3.2 Instrument and apparatus.....	14
3.3 Procedure.....	15
3.3.1 Preparation of poly( <i>n</i> -butyl acrylate- <i>co</i> -methyl methacrylate) chitosan encapsulation.....	15
3.3.2 Monomer conversion and total solids content (TSC).....	16
3.3.3 Characterization of transmission electron microscope.....	16
3.3.4 Characterization of particle size and surface charge.....	17
3.3.5 Characterization of viscosity.....	17
3.3.6 Characterization of thermal property by differential scanning calorimetry.....	17
3.3.7 Atomic Force Microscopy.....	18
3.3.8 Nuclear magnetic resonance.....	18
3.3.9 Surface tension.....	18
3.3.10 Bending test.....	19
CHAPTER IV RESULTS AND DISCUSSION.....	20
4.1 Monomer conversion and total solids content (TSC).....	20
4.2 Particle Morphology.....	24
4.3 Characterization of particle size and surface charge.....	27

	Page
4.4 Characterization of viscosity.....	34
4.5 Characterization of nuclear magnetic resonance.....	37
4.6 Atomic force microscopy.....	49
4.7 Bending Test .....	55
4.8 Different scanning calorimetry.....	57
CHAPTER V CONCLUSION.....	60
5.1 Conclusion.....	60
References.....	62
Appendices.....	65
Vita.....	79

## LIST OF TABLES

Table	Page
3.1 The formation of P( <i>n</i> -BA- <i>co</i> -MMA) particles encapsulated with chitosan.....	15
4.1 Monomer conversion and total solid contents of P( <i>n</i> -BA- <i>co</i> -MMA) particles with different monomer ratios.....	21
4.2 Monomer conversion of P( <i>n</i> -BA- <i>co</i> -MMA) particles encapsulated with various molecular weights and concentrations of chitosan.....	22
4.3 Total solids content of P( <i>n</i> -BA- <i>co</i> -MMA) ) particles encapsulated with various molecular weights and concentrations of chitosan.....	23
4.4 Average particle size and zeta potential of P( <i>n</i> -BA- <i>co</i> -MMA) with different monomer ratios.....	28
4.5 Average particle size and zeta potential of P( <i>n</i> -BA- <i>co</i> -MMA) with different monomer ratios and chitosan molecular weights (0.5%w/v).....	29
4.6 Grafting percentage of copolymer (1:1) encapsulated with 0.5% wt of various molecular weights of chitosan.....	48
4.7 Grafting percentage of copolymer (1:1) encapsulated with various chitosan concentrations.....	48
4.8 Grafting percentage of encapsulated copolymers prepared with various monomer ratios.....	49
4.9 Roughness of P( <i>n</i> -BA- <i>co</i> -MMA) at 1:1 monomer ratio encapsulated with different chitosan concentrations and molecular weights.....	54
4.10 Effect of chitosan concentration and molecular weight of P( <i>n</i> -BA- <i>co</i> -MMA) on the bending test.....	56
D.1 Surface tension of copolymers with different monomer ratios.....	71

Table	Page
D.2 Surface tension of encapsulated chitosan copolymers with different molecular weights (0.5%w/v).....	72
D.3 Surface tension of encapsulated chitosan copolymers with different molecular weights (1%w/v).....	72
D.4 Surface tension of encapsulated chitosan copolymers with different molecular weights (1.5%w/v).....	73
E.1 Particle size and zeta potential of copolymers at 1:1 monomer ratio encapsulated with chitosan (1.5%w/v) with different initiator concentrations.....	74
F.1 Grafting percentage of copolymer (1:1) encapsulated with 0.5% w/v of various molecular weights of chitosan (from peak area of <sup>1</sup> H-NMR spectrum)....	77
F.2 Grafting percentage of copolymer (1:1) encapsulated with various chitosan concentrations (from peak area of <sup>1</sup> H-NMR spectrum).....	77
F.3 Grafting percentage of encapsulated copolymers prepared with various monomer ratios (from peak area of <sup>1</sup> H-NMR spectrum).....	78

## LIST OF FIGURES

Figure	Page
2.1 Structure of chitin.....	7
2.2 Structure of chitosan.....	8
2.3 Solubility of chitosan in diluted acid solution.....	8
3.1 Structure of butyl acrylate.....	13
3.2 Structure of methyl methacrylate.....	14
4.1 TEM micrographs of P( <i>n</i> -BA- <i>co</i> -MMA) particles encapsulated with chitosan (0.5%w/v, MW $1.2 \times 10^5$ Da).....	25
4.2 TEM micrographs of P( <i>n</i> -BA- <i>co</i> -MMA) at 1:1 monomer ratio with different chitosan concentrations and molecular weights staining with 2%PTA .....	26
4.3 Effect of chitosan concentration from 0% to 1.5% (w/v) on particle size of P( <i>n</i> -BA- <i>co</i> -MMA) at 1:1 monomer ratio with different chitosan molecular weights.....	30
4.4 Effect of chitosan concentration from 0% to 1.5% (w/v) on zeta potential of P( <i>n</i> -BA- <i>co</i> -MMA) at 1:1 monomer ratio with different chitosan molecular weights.....	32
4.5 Effect of pH on the particle size of the copolymer prepared at 1:1 monomer ratio and 1.5% (w/v) chitosan concentration with different chitosan molecular weights.....	32
4.6 Effect of pH on zeta potential of copolymer prepared at 1:1 monomer ratio...	33
4.7 Effect of pH on zeta potential of copolymer prepared at 1:1 monomer ratio and 1.5% (w/v) chitosan concentration with different chitosan molecular weights.....	33

Figure	Page
4.8 Viscosities of P( <i>n</i> -BA- <i>co</i> -MMA) with different monomer ratios.....	34
4.9 Viscosities of P( <i>n</i> -BA- <i>co</i> -MMA) at 1:1 monomer ratio with different chitosan concentrations (MW $1.2 \times 10^5$ Da).....	35
4.10 Viscosities of P( <i>n</i> -BA- <i>co</i> -MMA) at 1:1 monomer ratio with different chitosan concentrations (MW $3.7 \times 10^5$ Da).....	35
4.11 Viscosities of P( <i>n</i> -BA- <i>co</i> -MMA) at 1:1 monomer ratio with different chitosan concentrations (MW $8.5 \times 10^5$ Da).....	36
4.12 Viscosities of P( <i>n</i> -BA- <i>co</i> -MMA) at 1:1 monomer ratio and 1.5%(w/v) with different chitosan molecular weights.....	36
4.13 $^1\text{H-NMR}$ spectra of P( <i>n</i> -BA- <i>co</i> -MMA) at 1:1 monomer ratio.....	39
4.14 $^1\text{H-NMR}$ spectra of P( <i>n</i> -BA- <i>co</i> -MMA) at 1:1 monomer ratio encapsulated with chitosan (0.5% w/v, MW $3.7 \times 10^5$ Da).....	40
4.15 $^1\text{H-NMR}$ spectra of P( <i>n</i> -BA- <i>co</i> -MMA) at 1:1 monomer ratio encapsulated with chitosan (1% w/v, MW $3.7 \times 10^5$ Da).....	41
4.16 $^1\text{H-NMR}$ spectra of P( <i>n</i> -BA- <i>co</i> -MMA) at 1:1 monomer ratio encapsulated with chitosan (1.5% w/v, MW $3.7 \times 10^5$ Da).....	42
4.17 $^1\text{H-NMR}$ spectra of P( <i>n</i> -BA- <i>co</i> -MMA) at 1:1 monomer ratio encapsulated with chitosan (0.5% w/v, MW $1.2 \times 10^5$ Da).....	43
4.18 $^1\text{H-NMR}$ spectra of P( <i>n</i> -BA- <i>co</i> -MMA) at 1:1 monomer ratio encapsulated with chitosan (0.5% w/v, MW $8.5 \times 10^5$ Da).....	44

Figure	Page
4.19 <sup>1</sup> H-NMR spectra of P( <i>n</i> -BA- <i>co</i> -MMA) at 1:2 monomer ratio encapsulated with chitosan (0.5% w/v, MW $3.7 \times 10^5$ Da).....	45
4.20 <sup>1</sup> H-NMR spectra of P( <i>n</i> -BA- <i>co</i> -MMA) at 3:2 monomer ratio encapsulated with chitosan (0.5% w/v, MW $3.7 \times 10^5$ Da).....	46
4.21 <sup>1</sup> H-NMR spectra of P( <i>n</i> -BA- <i>co</i> -MMA) at 2:1 monomer ratio encapsulated with chitosan (0.5% w/v, MW $3.7 \times 10^5$ Da).....	47
4.22 AFM images of P( <i>n</i> -BA- <i>co</i> -MMA) with different monomer ratios.....	50
4.23 AFM images of P( <i>n</i> -BA- <i>co</i> -MMA) at 1:1 monomer ratio encapsulated with different chitosan concentrations ( $3.7 \times 10^5$ Da) .....	52
4.24 AFM images of P( <i>n</i> -BA- <i>co</i> -MMA) at 1:1 monomer ratio encapsulated with different chitosan molecular weights (0.5%w/v).....	53
4.25 DSC thermograms of P( <i>n</i> -BA- <i>co</i> -MMA) prepared with different monomer ratios.....	58
4.26 DSC thermogram of chitosan at 1%w/v (MW $3.7 \times 10^5$ Da).....	58
4.27 DSC thermogram of P( <i>n</i> -BA- <i>co</i> -MMA) at 1:1 monomer ratio encapsulated with chitosan (1%w/v, MW $3.7 \times 10^5$ Da).....	59
A.1 Viscosities of P( <i>n</i> -BA) and PMMA.....	66
A.2 Viscosities of P( <i>n</i> -BA- <i>co</i> -MMA) with different monomer ratios and 1%(w/v) chitosan concentration (MW $1.2 \times 10^5$ Da).....	66
A.3 Viscosities of P( <i>n</i> -BA- <i>co</i> -MMA) with different monomer ratios and 1%(w/v) chitosan concentration (MW $3.7 \times 10^5$ Da).....	67
A.4 Viscosities of P( <i>n</i> -BA- <i>co</i> -MMA) in different monomer ratios and 1%(w/v) chitosan concentration (MW $8.5 \times 10^5$ Da).....	67

Figure	Page
B.1 AFM images of P( <i>n</i> -BA- <i>co</i> -MMA) with different monomer ratios encapsulated with chitosan (0.5% w/v, MW $1.2 \times 10^5$ Da).....	68
C.1 DSC thermograms of P( <i>n</i> -BA- <i>co</i> -MMA) prepared with different monomer ratios.....	69
C.2 DSC thermograms of P( <i>n</i> -BA- <i>co</i> -MMA) prepared at various monomer ratios encapsulated with 1%w/v, MW $3.7 \times 10^5$ Da.....	69
C.3 DSC thermograms of P( <i>n</i> -BA- <i>co</i> -MMA) at 1:1 monomer ratio encapsulated with different molecular weights of chitosan (1%w/v).....	70
D.1 Surface tension of copolymers with different monomer ratios.....	71
D.2 Surface tension of encapsulated chitosan copolymers with different molecular weights (0.5%w/v).....	72
D.3 Surface tension of encapsulated chitosan copolymers with different molecular weight (1%w/v).....	72
D.4 Surface tension of encapsulated chitosan copolymers with different molecular weights (1.5%w/v).....	73
E.1 AFM images of P( <i>n</i> -BA- <i>co</i> -MMA) at 1:1 monomer ratio encapsulated with chitosan (1.5% w/v, MW $3.7 \times 10^5$ Da) with different initiator concentrations.....	75
F.1 $^1\text{H}$ -NMR spectrum of P( <i>n</i> -BA- <i>co</i> -MMA) at 1:1 monomer ratio encapsulated with chitosan (0.5%w/v, MW $3.7 \times 10^5$ Da).....	76

# CHAPTER I

## INTRODUCTION

### 1.1 Scientific rationale

Emulsion polymerization is frequently used in industry to produce latex paints, rubbers, coatings and adhesives. Emulsion polymerization is a free radical polymerization performed in a heterogeneous reaction system, yielding submicron solid polymer particles dispersed in an aqueous medium. Emulsion polymerization has some clear advantages as compared to other types of free radical polymerization, being bulk, solution and suspension polymerizations. These advantages are a relatively high reaction rate, a moderate viscosity increase for high solids polymerization and a relatively good control of heat transfer.

In present, chitosan can be used in various applications such as medical, pharmaceutical, environmental, agriculture, and binder industry. Because chitosan is a biocompatible, non-toxic, and biodegradable natural polymer. Furthermore, chitosan has a good property in antibacterial. Since chitosan has amino group, made soluble in acidic solution and reactive with metal ion. In emulsion polymerization, chitosan acts as a surfactant. Chitosan adsorption to droplet surfaces can be either detrimental or beneficial to emulsion stability depending on the preparation conditions.

## 1.2 Objectives

1. To prepare poly(*n*-butyl acrylate-*co*-methyl methacrylate), (P(*n*-BA-*co*-MMA)) particles encapsulated with chitosan.

2. To study influence of molecular weight and concentration of chitosan on the colloidal and physical properties of P(*n*-BA-*co*-MMA) particles encapsulated with chitosan.

## 1.3 Scope and work plan

For this study, the particles of copolymer containing softy monomer (*n*-butyl acrylate) and hard monomer (methyl methacrylate) are prepared at various monomer ratios with different molecular weights, and concentrations of chitosan. The effect of these parameters on chitosan encapsulation efficiency is investigated. Copolymer particles with chitosan encapsulation are characterized as follows: particle size, zeta potential, viscosity, surface tension, and particle morphology. Film properties, such as  $T_g$ , surface roughness, and film flexibility are also studied.

## 1.4 Expected benefit

To find a suitable preparation condition for P(*n*-BA-*co*-MMA) particles encapsulated with various molecular weights and concentrations of chitosan.

## CHAPTER II

### THEORY AND LITERATURE REVIEW

#### 2.1 Emulsion polymerization

Emulsion polymerization is a free-radical-initiated chain polymerization in which a monomer or a mixture of monomers is polymerized in the presence of an aqueous solution of a surfactant to form a product, known as a latex. The latter is defined as a colloidal dispersion of polymer particles in an aqueous medium. The main ingredients for producing these polymerizations include, in addition to the monomer and water, surfactant, initiator, and chain transfer agent.[1] The main locus of polymerization is within the monomer-swollen latex particle, which are either formed at the start of polymerization or may be added initially (in which case one contains a seeded emulsion polymerization). The fact that particles in an emulsion polymerization are small, much smaller than those in a (conventional) emulsion, indicates that polymerization does not occur in the monomer droplets. If a surfactant is used above the critical micelle concentration (CMC), in the system, then micelle form. A micelle is an aggregate of  $\sim 10^2$  surfactant molecules, usually spherically shaped with the dimension of a few nanometers. One of the advantages of emulsion polymerization is the excellent heat exchange due to the low viscosity of the continuous phase during the whole reaction. Examples of applications are paints, coating, adhesives, finishes, and floor polishes. Emulsion polymerization is frequently used to create core-shell particles, which have a layer structure. Core-shell products

are in use by the coating industry, in photographic and printing materials, and in the production of high impact materials (a core of rubbery polymer and a shell of glassy engineering plastic).

Emulsion polymerization kinetics have important differences from solution and bulk polymerizations. These differences can lead to many advantages: for example, an increase in molar mass can be achieved without reducing the rate of polymerization. Emulsion polymerization is known for its relatively high rates of polymerization and high molar masses as compared to other polymerization techniques. A disadvantage of emulsion polymerization is the presence of surfactant and other additives, which may result in deleterious properties under some circumstances.[2]

### **2.1.1 Ingredients in recipes**

This section provides an overview of the major ingredients in emulsion polymerization. A laboratory scale recipe for an emulsion polymerization contains monomer, water, initiator, surfactant, and sometimes a buffer and/or chain transfer agents (CTAs). Commercial emulsion polymerization recipes are usually much more complicated, with 20 or more ingredients. The complexity of components, and the sensitivity of the system kinetics, mean that small changes in recipe or reaction conditions often result in unacceptable changes in the quality of the product formed.

### **2.1.2 Monomers**

Particles in an emulsion polymerization comprise largely monomers with a limited solubility in water. The most common monomers are styrene, butadiene, vinyl acetate, acrylates and methacrylates, acrylic acid and vinyl chloride. Besides monomers that make up a large part of the latex, other monomers are often added in smaller quantities and have specific functions, such as stabilization ((meth)acrylic acid) and reactivity in crosslinking (epoxy group containing monomers, amine- or hydroxyl-functional groups etc.), these are denoted 'functional monomers'.

### **2.1.3 Initiators**

The most frequently used initiators are the salts of peroxydisulfate. Sodium, potassium and ammonium salts are generally interchangeable and are used in the temperature range 50-90°C [1]. In cases where the polymerization should be performed at lower temperature (<50°C), a redox system can be used.

### **2.1.4 Surfactants**

A surfactant (surface active agent), also referred to as emulsifier, soap or stabilizer, is a molecule having both hydrophilic and hydrophobic segments. The general name for this group is amphipathic, indicating the molecules' tendency to arrange themselves at oil-water interfaces. In emulsion polymerization, surfactants

serve three important purposes: stabilization of the monomer droplets, generation of micelles, and stabilization of the growing polymer particles leading to a stable end product.

Surfactants are mostly classified according to the hydrophilic group:

- Anionic surfactants, where the hydrophilic part is an anion.
- Cationic surfactants, where the hydrophilic part is a cation.
- Amphoteric surfactants, where the properties of the hydrophilic function depend on the pH.
- Non-ionic surfactants, where the hydrophilic part is a non-ionic component, for instance polyols, sugar derivatives or chains of ethylene oxide.

Other types of surfactants are the polymeric (steric) stabilizers, such as partially hydrolysed polyvinyl acetate. Also oligomeric species formed in situ, when  $\text{SO}_4^{\cdot-}$  radicals react with some monomer units in the aqueous phase, will have surface active properties, and can even form a colloidally stable latex.

## **2.2 Core-shell morphologies**

The design of the core-shell particles are dictated by the desired properties and applications. The properties that core-shell latex particles exhibit depend on a number of parameters, such as the polymer or copolymer type, the molar mass, the amount of grafted material between the core and the shell material, the glass transition temperature ( $T_g$ ) of the polymer in the core and in the shell [2].

### 2.3 Chitin

Chitin is a cellulose-link biopolymer consisting of unbranched chains of predominantly  $\beta$ -(1,4)-2-acetamido-2-deoxy-D-glucopyranose (also named *N*-acetylglucosamine) residues. Its structure is shown in Figure 2.1. It does not dissolve in standard polar and non-polar solvents.[3] It is found particularly in the shells of crustaceans such as crab and shrimp, the cuticles of insects, and the cell walls of fungi.

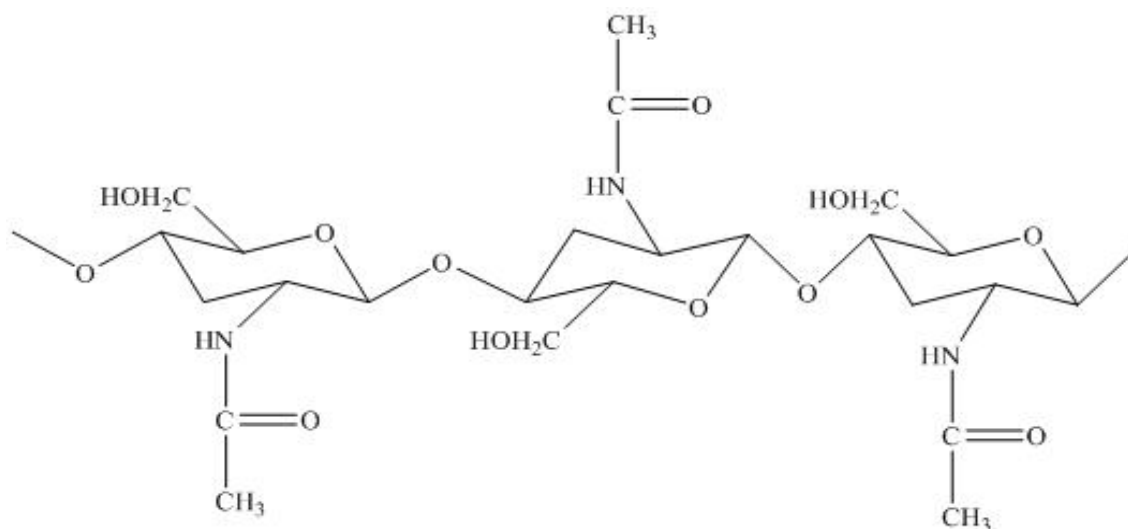


**Figure 2.1 :** Structure of chitin.

### 2.4 Chitosan

Chitosan, a  $\beta$ -(1,4)-2-amino-2-deoxy-D-glucopyranose, is a deacetylated form of chitin. Obtained from the shells of crabs, shrimps and other crustaceans, chitosan is a non-toxic, biodegradable and biocompatible natural polymer [4] that has many

potential applications in food, cosmetics, and pharmaceutical industries because of its unique nutritional and physiochemical properties. At relatively low pH ( $\text{pH} < 6.5$ ), chitosan is positively charged and tends to be soluble in dilute aqueous solutions, but at higher pH, it tends to lose its charge and may precipitate from solution due to deprotonation of the amino groups. Chitosan has also been shown to be capable of adsorbing to the surfaces of lipid droplets. Chitosan adsorption to droplet surfaces can be either detrimental or beneficial to emulsion stability depending on the preparation conditions, such as droplet concentration, droplet charge, droplet size, chitosan

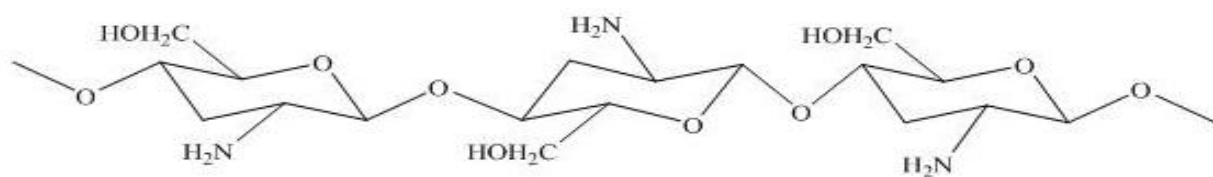


**Figure 2.2:** Structure of chitosan.

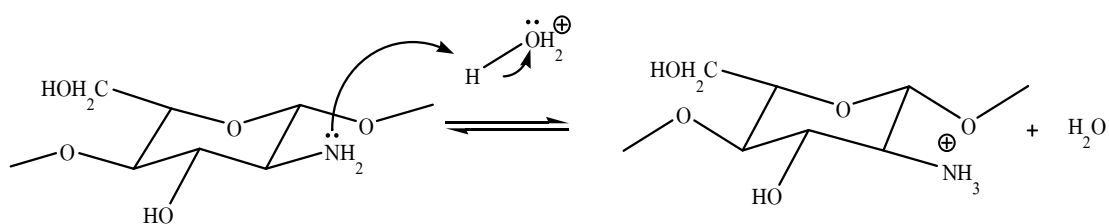


**Figure 2.3:** Solubility of chitosan in diluted acid solution.

## 2.5 Binder

The main functions of binder are to bind the pigment particles together and to bind to the substrate. There are two different types of binders, water soluble binders and latex binders. The most commonly used latex binder is styrene-butadiene followed by styrene-*n*-butyl acrylate (SA-latex), and polyvinylacetate (PVAc). In addition to its binding properties, the water soluble binder is also a thickener and water retention agent. The later properties are usually the most important for the water soluble binder. If a latex binder is used, a co-binder is usually added in order to control the water retention. The most commonly used water soluble binders are starch and the sodium salt of carboxymethylcellulose (NaCMC). Polyvinyl alcohol (PVA), alkali swellable polyacrylates and associative thickeners are other less used water-soluble binders. [6]

## 2.6 Liturature Reviews

Li et.al. [7] studied the novel method to prepare amphiphilic core-shell polymer nanospheres via graft copolymerization of methyl methacrylate from water-soluble polymer chains containing amino groups. Grafting reaction with bovine serum albumin (BSA), casein, and poly(allylamine) (PAA) generated nanospheres less than 100 nm in diameter. The particle size and stability depended on the structure and molecular weight of the hydrophilic polymer.

Ye et.al. [4] studied the novel core-shell particles with poly(*n*-butyl acrylate) cores and chitosan shells as an antibacterial coating for textiles. The core-shell

particles were prepared via a surfactant-free emulsion polymerization. Core-shell particles had a narrow size distribution with average particle diameter about 300 nm and showed highly positive surface charges. The treatment of cotton with PBA-chitosan particles conferred the fabric with excellent antibacterial property.

Tiğli and Evren [8] synthesized and characterized of pure polyacrylate latexes in which methyl methacrylate was used as the main monomer. The copolymer of P(MMA/MA) 1:3, P(MMA/EA) 1:1.5, and P(MMA/BA) 1:1 were prepared. Particle size of the selected copolymers was determine between 93.1 and 127.6 nm. Surface charge densities of the selected three copolymers were varied between 2.25 and 3.74  $\mu\text{C}/\text{cm}^2$ . P(MMA/EA) 1:1.5 copolymer was found to have satisfactory mechanical properties and excellent film forming ability.

Xue et.al. [9] studied the preparation and application of nanoscale microemulsion as binder for fabric inkjet printing. Microemulsion polymerization was synthesized with soft monomer (butyl acrylate, BA)/hard monomer (methyl methacrylate, MMA) at ratio as high as 8:1 (by weight), *N*-methylolacrylamide (NMA) as the crosslinking agent and monododecyl maleate (MDM) as a copolymerizable surfactant. The stability of the latex was greatly enhanced. The results indicated that the microemulsion had a number-average particle diameter less than 50 nm and with narrow size distribution. Fabrics printed by the inks prepared from the microemulsion exhibited excellent fabric colour fastnesses, good softness, and minor changes of the toughness after printing.

Nunes et. al. [10] examined the electrokinetic behavior of a poly(butyl acrylate-*co*-methacrylic acid) latex via emulsion polymerization, using sodium persulfate as the initiator, and sodium dodecyl sulfate as the surfactant. The presence

of carboxyl groups on the latex surface, as a consequence, seems to play an important role in the stability of the latex particles, since electrostatic repulsion between these negatively charged groups results in an electrically-driven stabilization of the dispersion. Zeta potential of the particles is the negative charge for all values. It is expected, since the surfactant used in this work was anionic nature.

Ogawa et. al. [11] studied the preparation and characterization of o/w emulsions containing cationic droplets stabilized with lecithin-chitosan membranes using two-stage process. A primary emulsion was prepared by homogenizing corn oil, lecithin, and acetic acid. This emulsion was diluted with chitosan solutions to form secondary emulsions. The electrical charge on the droplets increased from -49 to +54 mV as the chitosan concentration was increased from 0 to 0.04 wt%, which indicated the chitosan adsorption to the droplet surfaces. The emulsions became unstable to creaming when the chitosan concentration exceeded 0.008 wt%, which was attributed to charge neutralization and bridging flocculation effects.

Mun et.al. [12] studied the effect of molecular weight and degree of deacetylation of chitosan on the formation of oil-in-water emulsions stabilized by surfactant-chitosan membranes. The emulsion was prepared by homogenizing corn oil and aqueous surfactant solution. The influence of the molecular characteristics of chitosan on the properties of these emulsions was examined by using chitosan with different molecular weights and degrees of deacetylation. In the presence of 0.01 to 0.04 wt% chitosan, large clumps were observed at the top of emulsions. These clumps were clearly visible to the human eye and were a yellowish-brown color. At low molecular weight of chitosan, the zeta potential remained negative ( $\approx -10$  mV) at all chitosan concentrations, which suggested that the chitosan molecule did not adsorb to

the droplet surfaces. The zeta potential of chitosan at middle molecular weight and high molecular weight reached a relatively constant positive value ( $\sim +50$  to  $+60$  mV) when the chitosan concentration exceeded 0.05 wt%.

Kim et.al. [13] prepared the retinol-encapsulated low molecular water-soluble chitosan nanoparticles for application of cosmetic and pharmaceutical. Retinal-encapsulated chitosan nanoparticles have spherical shape and particle sizes were around 50-200 nm according to the contents of retinol. In FT-IR analysis, specific peak of chitosan at  $1590\text{ cm}^{-1}$  was devided to semi-droplet due to the electrostatic interaction between amino group of chitosan and hydroxyl group of retinol. From  $^1\text{H-NMR}$  spectra, specific peaks both of retinol and chitosan was appeared with  $\text{D}_2\text{O/DMSO}$  (1/4, v/v) mixture. From HPLC studied, the retinol was stably encapsulated into the chitosan nanoparticles and maintained their peculiar properties.

## CHAPTER III

### EXPERIMENTAL

#### 3.1 Chemicals

##### 3.1.1 *n*-butyl acrylate (*n*-BA)

*n*-Butyl acrylate was purchased from Fluka, Germany. The inhibitor was removed using a column packed with aluminium oxide.



**Figure 3.1** : Structure of butyl acrylate.

##### 3.1.2 Methyl methacrylate (MMA)

Methyl methacrylate was purchased from Aldrich, Germany. The inhibitor was removed using a column packed with aluminium oxide.

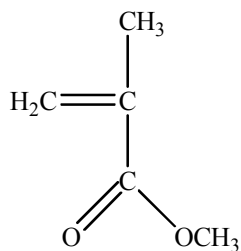


**Figure 3.2 :** Structure of methyl methacrylate.

### 3.1.3 Chitosan

Three molecular weights of chitosan ( $1.2 \times 10^5$ ,  $3.7 \times 10^5$  and  $8.5 \times 10^5$  Da, 87-88% deacetylation) were obtained from Koyo Chemical, Japan.

### 3.1.4 Potassium persulphate (KPS)

Potassium persulphate was purchased from Ajax Finechem, Australia

## 3.2 Instrument and Apparatus

Instruments and apparatus for the research are as follows:

1. Transmission electron microscope (JEOL, JEM-2100, Japan)
2. Viscometer (Brookfield, Model DV-III, Germany)
3. Nano-sizer (Malvern Instrument, Zetasizer Nano Series, Germany)
4. Differential scanning calorimeter (Perkinelmer, Diamond Pyris 7, U.S.A)

5. Scanning probe microscope (Veeco, Nanoscope IV, Germany)
6. Nuclear magnetic resonance spectrometer ( Varian, INOVA, U.S.A)
7. Surface tension meter (Krüss, K6, Germany)

### 3.3 Procedure

#### 3.3.1 Preparation of P(*n*-BA-*co*-MMA) particles encapsulated with chitosan

P(*n*-BA-*co*-MMA) particles encapsulated with chitosan were synthesized by emulsion polymerization. A 250 mL round-bottomed, four-necked flask equipped with a condenser, a teflon stirrer, and nitrogen inlet was immersed in a water bath with a control temperature at 80°C. Chitosan solutions which were prepared at 0.5%, 1%, and 1.5%w/v by dissolving the chitosan in 1%v/v acetic acid solution were added into the flask. The monomers were added afterward. The mixture was purged with nitrogen for 30 min. Next, a solution of potassium persulphate at 0.1 wt% was added, and the mixture was heated at 80°C for 2 hours under nitrogen atmosphere.

**Table 3.1** The formation of P(*n*-BA-*co*-MMA) particles encapsulated with chitosan

chemicals	contents
<i>n</i> -BA : MMA	1:2, 1:1, 3:2, 2:1
chitosan FL80 FM80 FM40	0.5, 1.0, 1.5%w/v
KPS	0.1%w/v

### 3.3.2 Monomer conversion and total solids content (TSC)

Monomer conversion and total solids content were determined by gravimetric analysis method. The sample was first weighed, and then evaporated at room temperature and ovened at 60°C, until a constant weight was obtained. The conversion and total solids content were calculated according to equations (1) and (2):

$$\text{Conversion (\%)} = \frac{W_p - W_s - W_i}{W_t} \times 100 \quad (1)$$

$$\text{TSC (\%)} = \frac{W_p}{W_t} \times 100 \quad (2)$$

Where  $W_p$  is the weight of polymer,  $W_s$  the weight of surfactant or chitosan,  $W_i$  the weight of initiator,  $W_t$  the total weight of monomers used in the synthesis, and  $W_l$  the weight of latex.[7]

### 3.3.3 Characterization of transmission electron microscope

The dilute latex solution was dropped on a carbon-coated grid. Upon drying, it was stained with a small drop of 2% phosphotungstic acid (PTA) and dried at room temperature before analysis.

### **3.3.4 Characterization of particle size and surface charge**

The sample was diluted with DI water at different pH values before measurement. Each sample was repeatedly measured for three times. All measurements were done at 25°C with an angle detection of 90°.

### **3.3.5 Characterization of viscosity**

Brookfield rotating viscometer was maintained at a constant temperature of 25°C by water bath. The shear rate was varied from 198 to 330 s<sup>-1</sup>.

### **3.3.6 Characterization of thermal property by differential scanning calorimetry (DSC)**

The sample of 10 mg was accurately weighed into an aluminum pan and sealed. An empty closed aluminum solid pan was used as a reference cell. The measurement was conducted at a constant heating rate of 10°C per minute over a temperature range of 0–350°C. An inert atmosphere was maintained by purging with nitrogen.

### **3.3.7 Atomic Force Microscopy (AFM)**

AFM experiment was carried out in order to photograph film formation property of P(*n*-BA-*co*-MMA) particles encapsulated with different molecular weights and concentrations of chitosan. The film was allowed to air-dry at ambient temperature for 7 days prior to measurement. AFM images were taken under tapping mode. Scanned images were of size  $1\mu\text{m} \times 1\mu\text{m}$ .

### **3.3.8 Nuclear magnetic resonance (NMR)**

The copolymer and copolymer with chitosan encapsulation were separately dissolved in  $\text{CDCl}_3$  and  $\text{CDCl}_3/\text{acetic acid-}d_4$ , respectively. The chitosan grafted copolymer was extracted with 1%v/v acetic acid solution for 16 hours to removed the adsorbed chitosan on the dry particles, and further extracted with chloroform for 16 hours. While homopolymers of P(*n*-BA) and PMMA were extracted with chloroform for 16 hours.

### **3.3.9 Surface tension**

The surface tension of latex was measured at room temperature. This method is based on the measurement of the force required to detach a frame, in this case a platinum ring, from the surface of the latex.

### **3.3.10 Bending test**

The bending test of the coating material was performed using ASTM D522-93a. The sample preparation was done by pouring the amount of 17 g of latex into an acrylic mold filled with aluminium sheet and ovened at 80°C for 3-4 hours. The coating material under test was applied at uniform thickness to a sheet metal. The procedure of testing is as follows: place the test panel over a mandrel with the uncoated side in contact and with at least 2 inch overhang on either side. Using a steady pressure of the fingers, bend the panel approximately 180° around the mandrel at a uniform velocity in a time of 1 second unless an alternative time is agreed upon between the panel immediately for cracking visible to the unaided eye. If cracking has not occurred, repeat the procedure using successively smaller diameter mandrels on previously untested areas of specimen until failure occurs or until the smallest diameter mandrel has been used. This test method has been useful in rating attached coating for their ability to resist cracking when elongated.

## CHAPTER IV

### RESULTS AND DISCUSSION

#### 4.1 Monomer conversion and total solid content (TSC)

Monomer conversion and total solids content (TSC) of the poly(*n*-butyl acrylate-*co*-methyl methacrylate), (P(*n*-BA-*co*-MMA) with different monomer ratios are obtained according to the equations (1) and (2), respectively, as seen in Table 4.1. The results show that %conversion of copolymer are achieved at high conversion, while % solids content is reached approximately at 13%wt, which is lower than the original added amount of 15%wt. This is probably due to monomer evaporation during the process, and the completed conversion could be reached at longer reaction time. The result of monomer conversion and total solid content (TSC) of P(*n*-BA-*co*-MMA) encapsulated with chitosan prepared at different monomer ratios and molecular weights and concentrations of chitosan are given in Tables 4.2 and 4.3, respectively. The results show that most at % solid content and monomer conversion of the chitosan encapsulation particles are obtained similar to the ones prepared without chitosan addition.

**Table 4.1** Monomer conversion and total solid content of P(*n*-BA-*co*-MMA) particles with different monomer ratios

Polymer *	%Monomer conversion	%TSC
P( <i>n</i> -BA- <i>co</i> -MMA) 1:2	88.8 ± 0.4	13.3 ± 0.04
P( <i>n</i> -BA- <i>co</i> -MMA) 1:1	86.7 ± 1.2	13.1 ± 0.01
P( <i>n</i> -BA- <i>co</i> -MMA) 3:2	86.5 ± 0.1	12.9 ± 0.02
P( <i>n</i> -BA- <i>co</i> -MMA) 2:1	85.1 ± 0.5	12.9 ± 0.08

\*The synthesis recipe contains SDS at 10 mM

**Table 4.2** Monomer conversion of P(*n*-BA-*co*-MMA) particles encapsulated with various molecular weights and concentrations of chitosan

Polymer	Monomer conversion (%)								
	$1.2 \times 10^5$ Da			$3.7 \times 10^5$ Da			$8.5 \times 10^5$ Da		
	0.5	1	1.5	0.5	1	1.5	0.5	1	1.5
P( <i>n</i> -BA- <i>co</i> -MMA) 1:2	88.3 ± 0.3	85.4 ± 0.2	87.9 ± 0.3	92.7 ± 0.5	90.7 ± 0.3	71.6 ± 0.1	89.3 ± 0.6	86.9 ± 0.2	87.9 ± 0.8
P( <i>n</i> -BA- <i>co</i> -MMA) 1:1	87.8 ± 0.4	88.9 ± 0.3	88.9 ± 0.4	88.5 ± 0.3	89.7 ± 0.04	90.7 ± 2.9	91.3 ± 0.8	90.4 ± 0.3	88.9 ± 1.3
P( <i>n</i> -BA- <i>co</i> -MMA) 3:2	89.6 ± 0.2	87.2 ± 0.2	76.6 ± 0.04	88.5 ± 1.4	88.3 ± 0.3	85.4 ± 1.0	87.5 ± 0.6	88.6 ± 0.2	89.1 ± 0.8
P( <i>n</i> -BA- <i>co</i> -MMA) 2:1	87.9 ± 0.5	88.2 ± 0.4	85.2 ± 0.2	88.0 ± 0.2	90.5 ± 0.08	76.8 ± 0.2	87.6 ± 0.8	87.6 ± 0.6	87.8 ± 1.2

**Table 4.3** Total solids content of P(*n*-BA-*co*-MMA) particles encapsulated with various molecular weights and concentrations of chitosan

Polymer	Total solid content (%)								
	$1.2 \times 10^5$ Da (%w/v)			$3.7 \times 10^5$ Da (%w/v)			$8.5 \times 10^5$ Da (%w/v)		
	0.5	1	1.5	0.5	1	1.5	0.5	1	1.5
P( <i>n</i> -BA- <i>co</i> -MMA) 1:2	12.1 ± 0.1	12.2 ± 0.02	13.1 ± 0.02	12.5 ± 0.02	12.2 ± 0.01	10.9 ± 0.01	12.5 ± 0.03	12.5 ± 0.17	12.7 ± 0.04
P( <i>n</i> -BA- <i>co</i> -MMA) 1:1	12.1 ± 0.02	12.7 ± 0.02	13.2 ± 0.02	12.3 ± 0.01	12.8 ± 0.01	13.4 ± 0.4	12.4 ± 0.01	12.7 ± 0.05	12.9 ± 0.03
P( <i>n</i> -BA- <i>co</i> -MMA) 3:2	12.3 ± 0.3	12.5 ± 0.01	12.5 ± 0.03	12.2 ± 0.2	12.7 ± 0.01	12.7 ± 0.1	12.2 ± 0.2	12.8 ± 0.03	12.7 ± 0.01
P( <i>n</i> -BA- <i>co</i> -MMA) 2:1	12.1 ± 0.02	12.5 ± 0.03	12.5 ± 0.01	12.1 ± 0.03	12.9 ± 0.02	11.6 ± 0.02	12.2 ± 0.04	12.6 ± 0.02	12.6 ± 0.03

## 4.2 Particle Morphology

TEM micrographs of P(*n*-BA-*co*-MMA) particles with chitosan encapsulation (Figure 4.1) indicate that the particles are spherical. Staining of the particles with 2% phosphotungstic acid (PTA) clearly revealed the chitosan layer surrounding the particles. It is noticeable that the chitosan layer gains more thickness when the amount of *n*-butyl acrylate is increased. While a thinner chitosan layer is present on PMMA particles. Moreover, at 1:1 monomer ratio, it is observed that the thickness of chitosan layer is increased when the chitosan concentration and molecular weight are increased as seen in Figure 4.2.

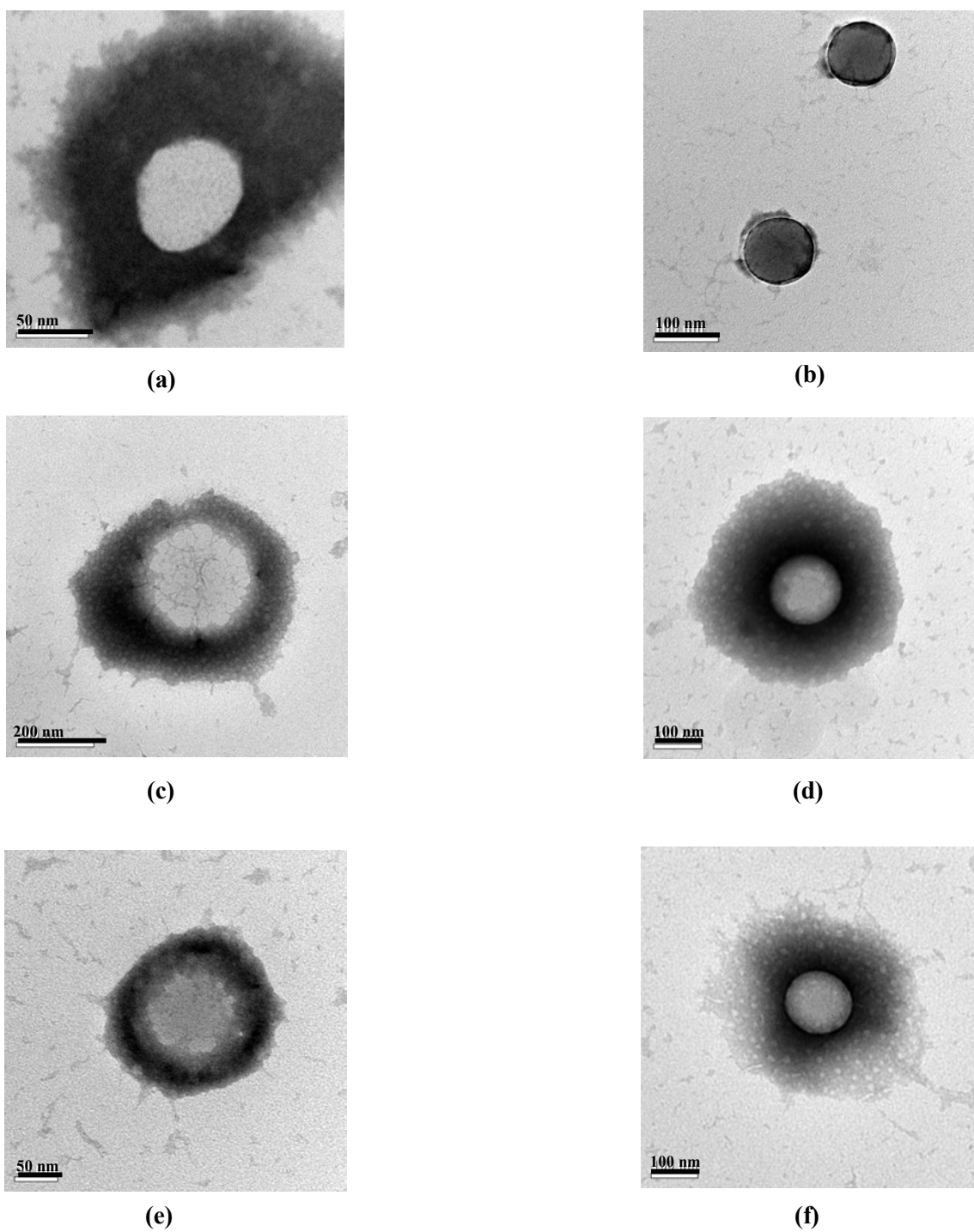


**Figure 4.1** : TEM micrographs of P(*n*-BA-*co*-MMA) particles encapsulated with chitosan (0.5%w/v, MW  $1.2 \times 10^5$  Da): (a) P(*n*-BA)/chitosan, (b) PMMA/chitosan, (c) P(*n*-BA-*co*-MMA) 2:1/chitosan, (d) P(*n*-BA-*co*-MMA) 3:2/chitosan, (e) P(*n*-BA-*co*-MMA) 1:1/chitosan, and (f) P(*n*-BA-*co*-MMA) 1:2/chitosan.

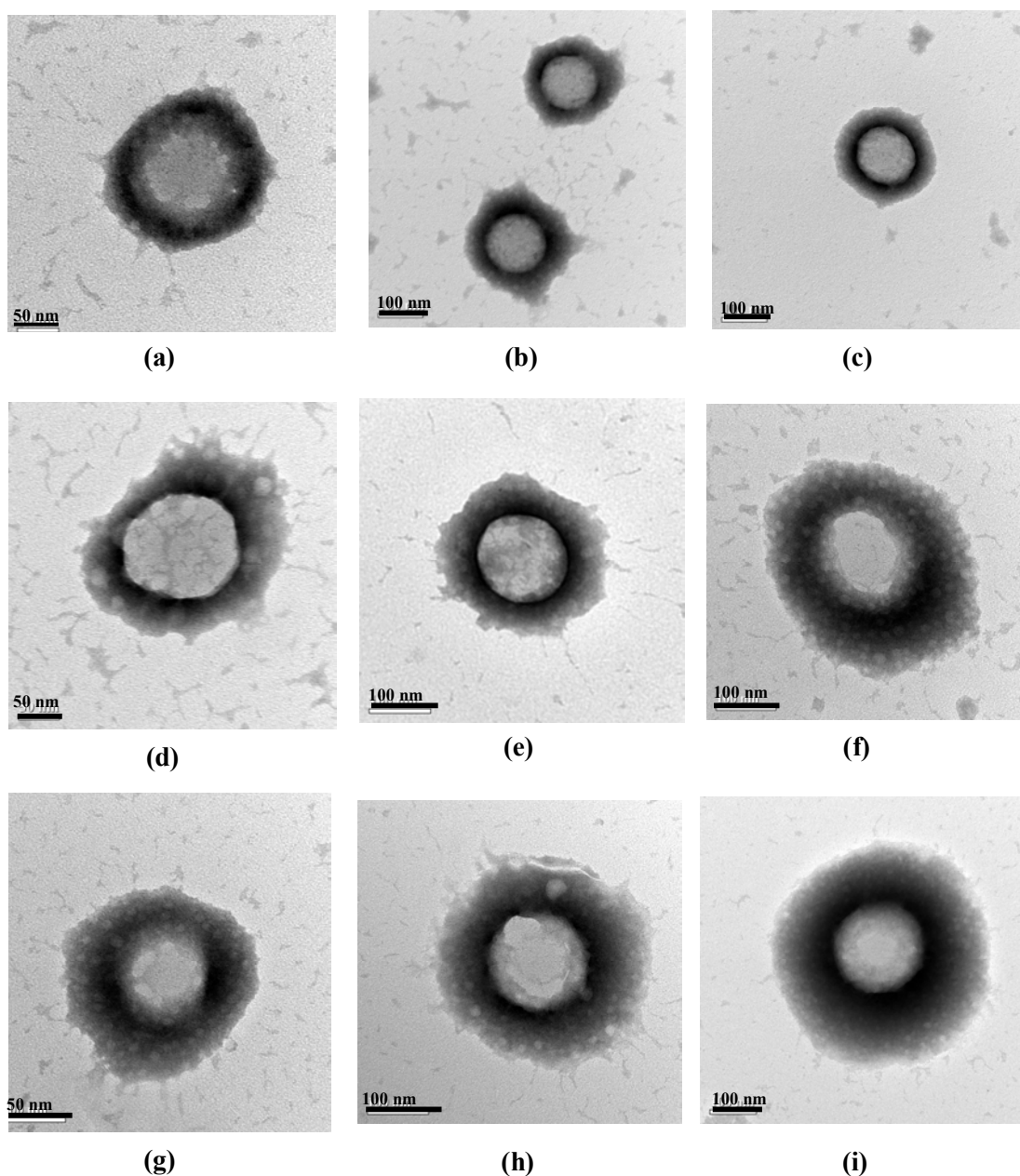


**Figure 4.2 :** TEM micrographs of P(*n*-BA-*co*-MMA) at 1:1 monomer ratio with different chitosan concentrations and molecular weights staining with 2%PTA: (a) 0.5% (MW  $1.2 \times 10^5$  Da), (b) 1% (MW  $1.2 \times 10^5$  Da), (c) 1.5% (MW  $1.2 \times 10^5$  Da), (d) 0.5% (MW  $3.7 \times 10^5$  Da), (e) 1% (MW  $3.7 \times 10^5$  Da), (f) 1.5% (MW  $3.7 \times 10^5$  Da), (g) 0.5% (MW  $8.5 \times 10^5$  Da), (h) 1% (MW  $8.5 \times 10^5$  Da), and (i) 1.5% (MW  $8.5 \times 10^5$  Da).

### 4.3 Characterization of particle size and surface charge

The average particle size and surface charge of P(*n*-BA-*co*-MMA) prepared at different monomer ratios with and without chitosan encapsulation were characterized by dynamic light scattering particle size analyzer (Malvern instrument Zetasizer). As it is seen in Table 4.4, the particle sizes prepared with various monomer ratios are obtained in proximity and rather small (in the range of 55-65 nm). This is probably due to a micellar nucleation that governs the emulsion polymerization since the surfactant concentration added is well above its CMC. While zeta potential of the particles appears to depend on the monomer ratio in which increasing in the amount of *n*-butyl acrylate yields a higher charge amount from surfactant adsorption on the particle surface. The fact that the solubility of MMA in water is 0.15 mol L<sup>-1</sup> (45°C) which is higher than that of BA (0.01 mol L<sup>-1</sup>, 45). It suggests that there is a polarity different between two monomers. When the polarity of monomer is higher in this case is MMA monomer, the tendency of surfactant molecule to be buried inside the particles is larger, resulting in smaller amount of adsorption and then lower charger density present on the particle surface. The highest zeta potential is observed at 1:1 (*n*-BA:MMA) monomer ratio. The result of particle size of the particles prepared with various monomer ratios and encapsulated with 0.5% wt of various molecular weights of chitosan. The particles obtained with chitosan encapsulation are obviously larger size than the ones without the encapsulation. It can also be seen that the copolymer prepared at 1:2 monomer ratio has the largest particle size followed by 3:2, 2:1, and 1:1 monomer ratios, respectively. The encapsulated particle size tends to decrease as the amount of BA is increased. As mentioned earlier, BA has lower water solubility compared with MMA. This result in a much smaller oligomer radical is formed during polymerization. Therefore, the

nucleation rate is enhanced, and particle diameter is thus smaller. [14] Besides the monomer ratio effect, the molecular weight of chitosan has also influenced on the particle size as well in which high molecular weight of chitosan can encapped more on the particles. This is seen when the copolymer is prepared with  $8.5 \times 10^5$  Da of chitosan, the largest particle size is obtained at any monomer ratio. With chitosan encapsulation, the positive charge is present on the particle surface (Table 4.5) because the amino groups ( $\text{NH}_2$ ) in the chitosan became cationic  $\text{NH}_3^+$  groups in the acid solution. At 0.5%wt addition of chitosan, higher molecular weight produces a slight increase in charge density on the particle surface. However, monomer ratio seems to have less effect on the particle charge, except at 1:1 monomer ratio. It is noticed that the encapsulation of the particle at 1:1 monomer ratio has the smallest size compared to other monomer ratios. This might influence on smaller amount of chitosan adsorption; thus the lowest zeta potential is obtained.

**Table 4.4** Average particle size and zeta potential of P(*n*-BA-*co*-MMA) with different monomer ratios

Polymer	Average Particle size (nm)	Zeta potential (mV)
P( <i>n</i> -BA- <i>co</i> -MMA) 1:2	56.9 ± 0.7	-38.1 ± 5.9
P( <i>n</i> -BA- <i>co</i> -MMA) 1:1	57.9 ± 0.2	-51.9 ± 2.2
P( <i>n</i> -BA- <i>co</i> -MMA) 3:2	61.5 ± 0.3	-41.6 ± 2.5
P( <i>n</i> -BA- <i>co</i> -MMA) 2:1	63.4 ± 0.6	-44.3 ± 1.9

**Table 4.5** Average particle size and zeta potential of P(*n*-BA-*co*-MMA) with different monomer ratios and chitosan molecular weights (0.5%w/v)

Polymer	Average Particle size (nm)	Zeta potential (mV)
P( <i>n</i> -BA- <i>co</i> -MMA) 1:2/0.5% (MW $1.2 \times 10^5$ Da)	$240.0 \pm 2.7$	$29.4 \pm 0.2$
P( <i>n</i> -BA- <i>co</i> -MMA) 1:1/0.5% (MW $1.2 \times 10^5$ Da)	$144.3 \pm 4.0$	$27.3 \pm 0.5$
P( <i>n</i> -BA- <i>co</i> -MMA) 3:2/0.5% (MW $1.2 \times 10^5$ Da)	$196.3 \pm 1.5$	$34.0 \pm 1.4$
P( <i>n</i> -BA- <i>co</i> -MMA) 2:1/0.5% (MW $1.2 \times 10^5$ Da)	$184.3 \pm 1.2$	$35.4 \pm 1.3$
P( <i>n</i> -BA- <i>co</i> -MMA) 1:2/0.5% (MW $3.7 \times 10^5$ Da)	$308.0 \pm 4.6$	$34.4 \pm 0.2$
P( <i>n</i> -BA- <i>co</i> -MMA) 1:1/0.5% (MW $3.7 \times 10^5$ Da)	$186.7 \pm 0.6$	$30.7 \pm 0.6$
P( <i>n</i> -BA- <i>co</i> -MMA) 3:2/0.5% (MW $3.7 \times 10^5$ Da)	$195.7 \pm 0.6$	$35.9 \pm 1.2$
P( <i>n</i> -BA- <i>co</i> -MMA) 2:1/0.5% (MW $3.7 \times 10^5$ Da)	$192.6 \pm 1.2$	$34.6 \pm 0.8$
P( <i>n</i> -BA- <i>co</i> -MMA) 1:2/0.5% (MW $8.5 \times 10^5$ Da)	$350.0 \pm 5.3$	$37.5 \pm 1.1$
P( <i>n</i> -BA- <i>co</i> -MMA) 1:1/0.5% (MW $8.5 \times 10^5$ Da)	$182.3 \pm 2.3$	$28.9 \pm 0.3$
P( <i>n</i> -BA- <i>co</i> -MMA) 3:2/0.5% (MW $8.5 \times 10^5$ Da)	$277.0 \pm 7.8$	$36.7 \pm 0.9$
P( <i>n</i> -BA- <i>co</i> -MMA) 2:1/0.5% (MW $8.5 \times 10^5$ Da)	$244.3 \pm 3.1$	$36.4 \pm 0.1$

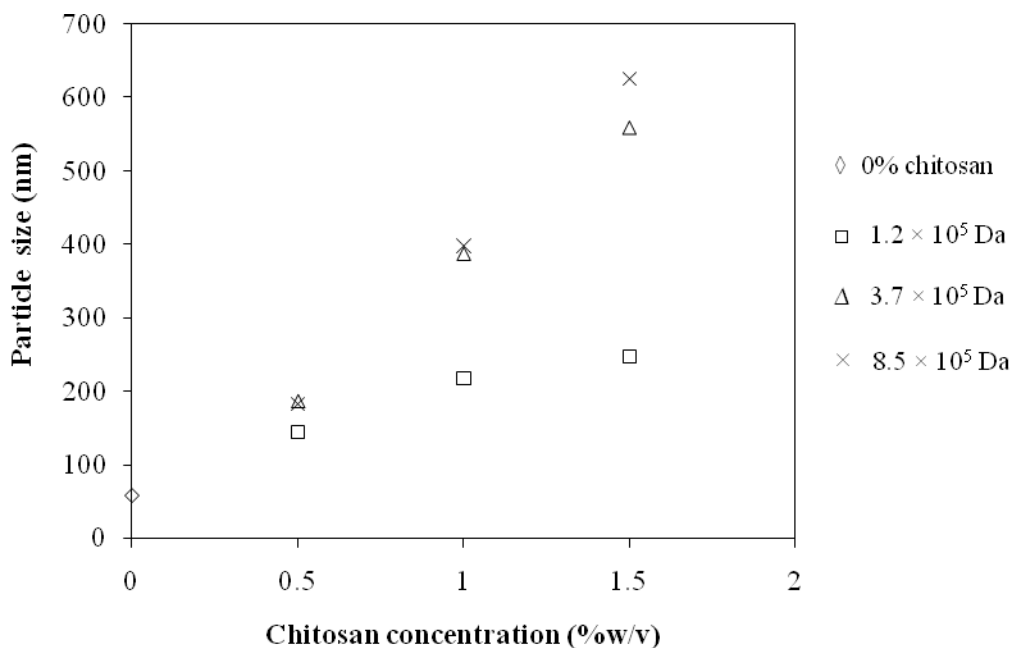


**Figure 4.3 :** Effect of chitosan concentration from 0% to 1.5% (w/v) on particle size of *P(n-BA-co-MMA)* at 1:1 monomer ratio with different chitosan molecular weights.

The effect of chitosan concentration from 0% to 1.5% (w/v) and molecular weight on particle is shown in Figure 4.3. The average particle size of *P(n-BA-co-MMA)* at 1:1 monomer ratio with high molecular weight of chitosan ( $8.5 \times 10^5$  Da) is the most affected by the chitosan concentration, and a linear relationship is obtained when the concentration of chitosan is increased.

Chitosan is a weak base polysaccharide, having an average amino group density of 0.837 per disaccharide unit, and insoluble at neutral and alkaline pH values. In acidic medium, the amino groups will be positively charged, conferring to the polysaccharide a high charge density. Therefore, the surface charge density of

chitosan molecule is strongly depending on pH of solution, and the ionic cross-linking process for the formation of chitosan/P(*n*-BA-*co*-MMA) particles is pH responsive, providing opportunities to modulate the formulation and property of the copolymer encapsulated with chitosan.[15] The zeta potential of copolymers with different chitosan concentrations and molecular weights is displayed in Figure 4.4. The electrical charge is raised when the chitosan concentration and molecular weight are increased. However, the chitosan concentration shows a strong effect on the zeta potential more than the molecular weight effect. The effects of changing environmental pH on nanoparticle size and zeta potential of P(*n*-BA-*co*-MMA) at 1:1 monomer ratio encapsulated with different molecular weights of chitosan (1.5%w/v) are shown in Figure 4.5 and Figure 4.7, respectively. The pH values of P(*n*-BA-*co*-MMA) at 1:1 monomer ratio encapsulated with chitosan have been adjusted to 3, 5, and 7. The zeta potential of the chitosan encapsulated particles is sensitive to pH in which the potential is decreased as pH is increased, suggesting that the surface density of protonised amino groups and degree of protonisation are reversibly responsive to changing solution pH values. Moreover, particle size and zeta potential at solution pH5 are very sensitive to the changing pH value of the residing aqueous environment, in which a reduction in both particle size and zeta potential are noticed, which is probably due to a decrease in protonated ions and simultaneous shrinkage of chitosan layer. An increase in measured average particle size could be caused mainly by particle aggregation when solution pH value is increased, rather than by further growth of the individual particle size after initial formation.[16]

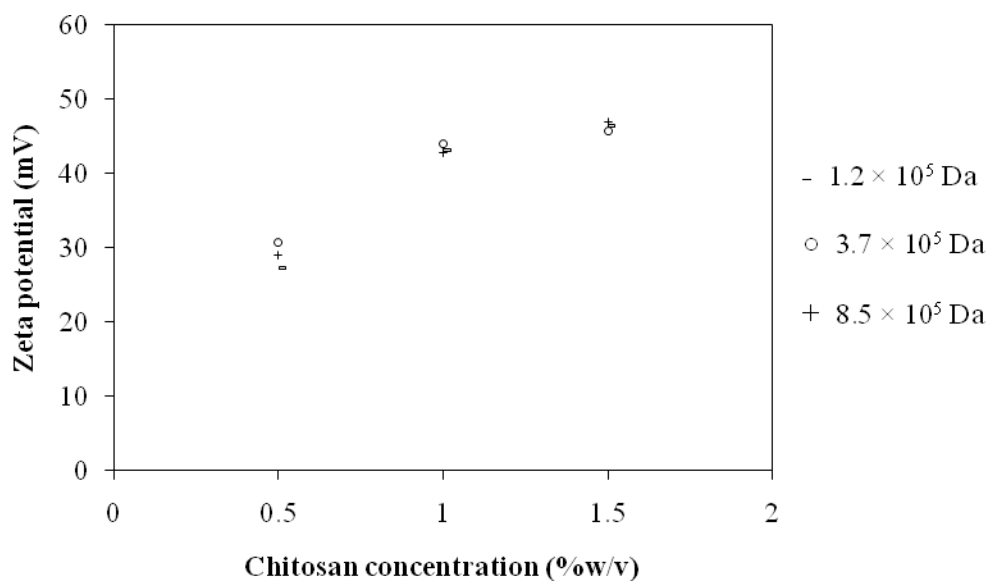


**Figure 4.4 :** Effect of chitosan concentration from 0% to 1.5% (w/v) on zeta potential of P(*n*-BA-*co*-MMA) at 1:1 monomer ratio with different chitosan molecular weights.

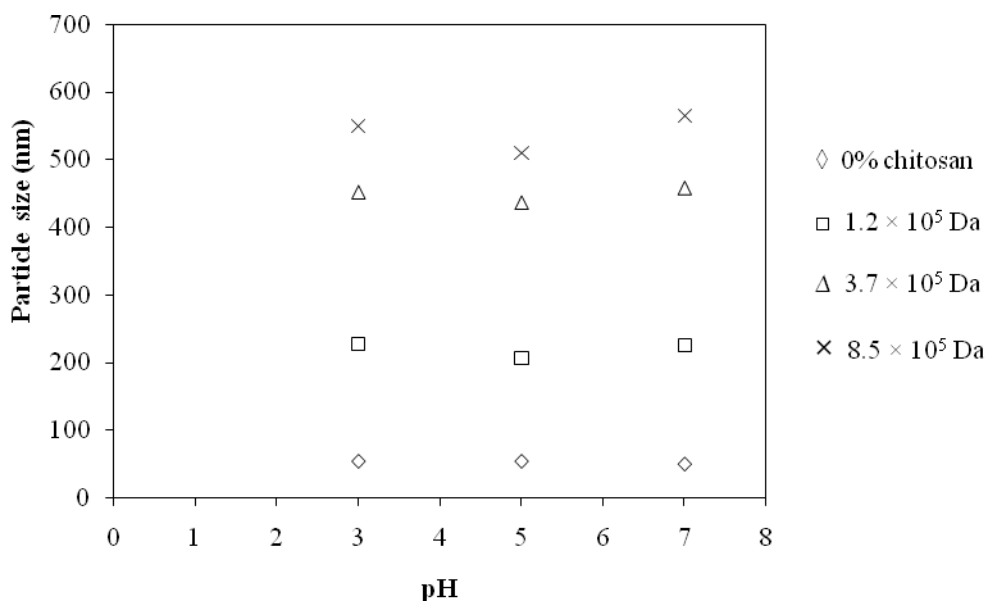


**Figure 4.5 :** Effect of pH on the particle size of the copolymer prepared at 1:1 monomer ratio and 1.5% (w/v) chitosan concentration with different chitosan molecular weights.

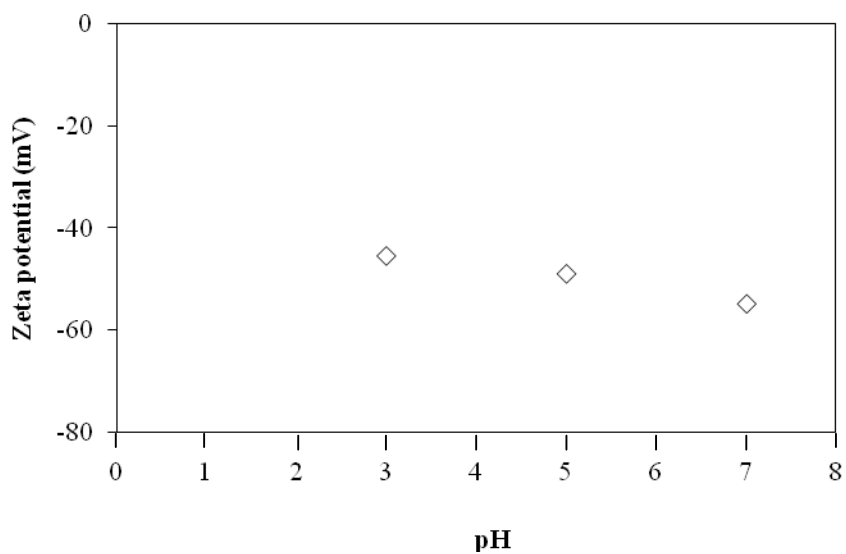


**Figure 4.6 :** Effect of pH on zeta potential of copolymer prepared at 1:1 monomer ratio.

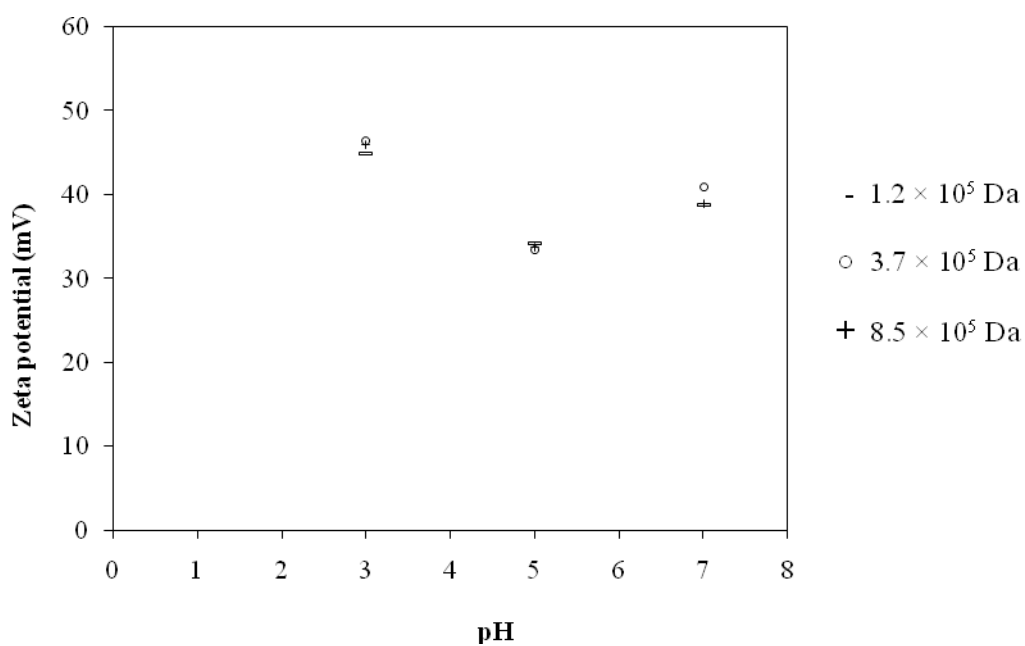


**Figure 4.7 :** Effect of pH on zeta potential of copolymer prepared at 1:1 monomer ratio and 1.5% (w/v) chitosan concentration with different chitosan molecular weights.

#### 4.4 Characterization of viscosity

Viscosities of the copolymers prepared with different monomer ratios are given in Figure 4.8, the viscosities of various P(*n*-BA-*co*-MMA) are decreased with increasing the contents of *n*-BA in monomer feed. They appear in close proximity, corresponding to similarity in particle size. When the particles are encapsulated, the viscosity of the emulsion is also enhanced. The effect is more pronounced at 1% wt and 1.5% wt of chitosan (Figures 4.9-4.12). High molecular weight of chitosan also influences on the viscosity of the particles. Since the large particle size is attained when the concentration and molecular weight of the chitosan are increased, generating high shear force passing through the particles, hence the viscosity is increased. Similar trends are obtained with other monomer ratios as included in Appendices.

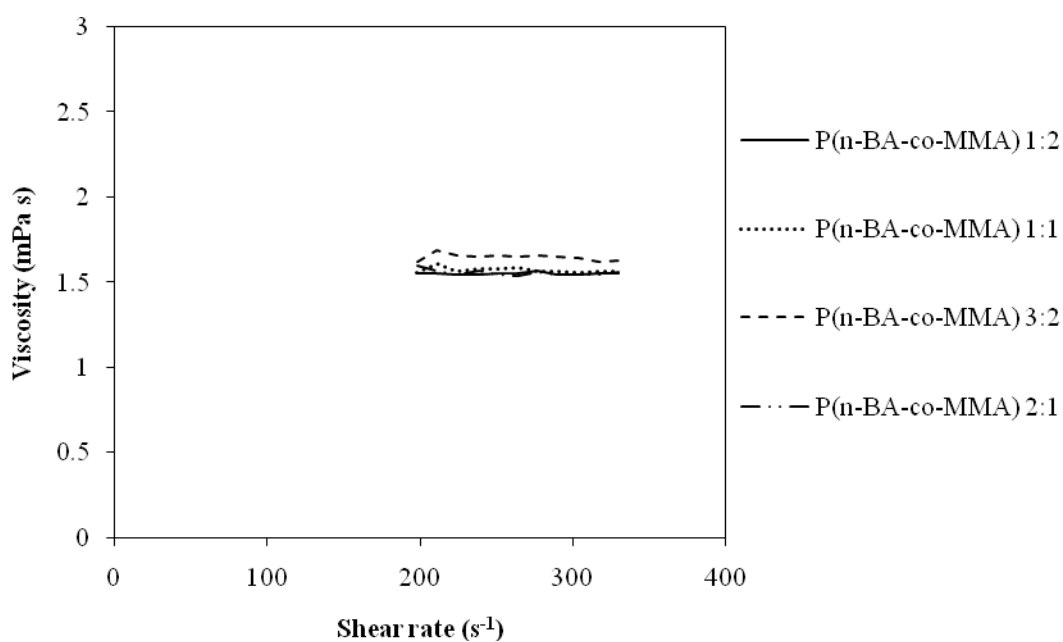


**Figure 4.8 :** Viscosities of P(*n*-BA-*co*-MMA) with different monomer ratios.

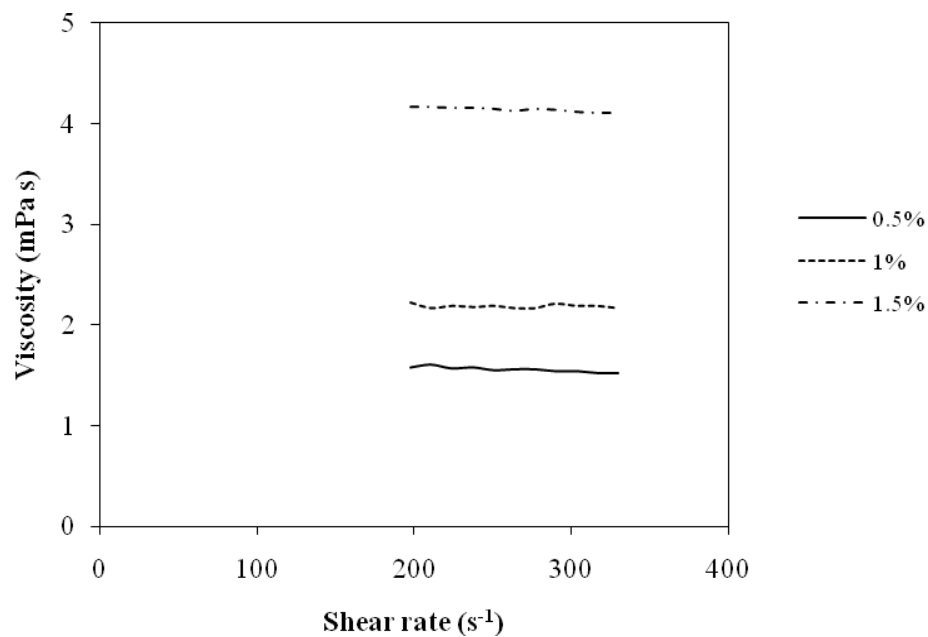


**Figure 4.9** : Viscosities of P(*n*-BA-*co*-MMA) at 1:1 monomer ratio with different chitosan concentrations (MW  $1.2 \times 10^5$  Da).

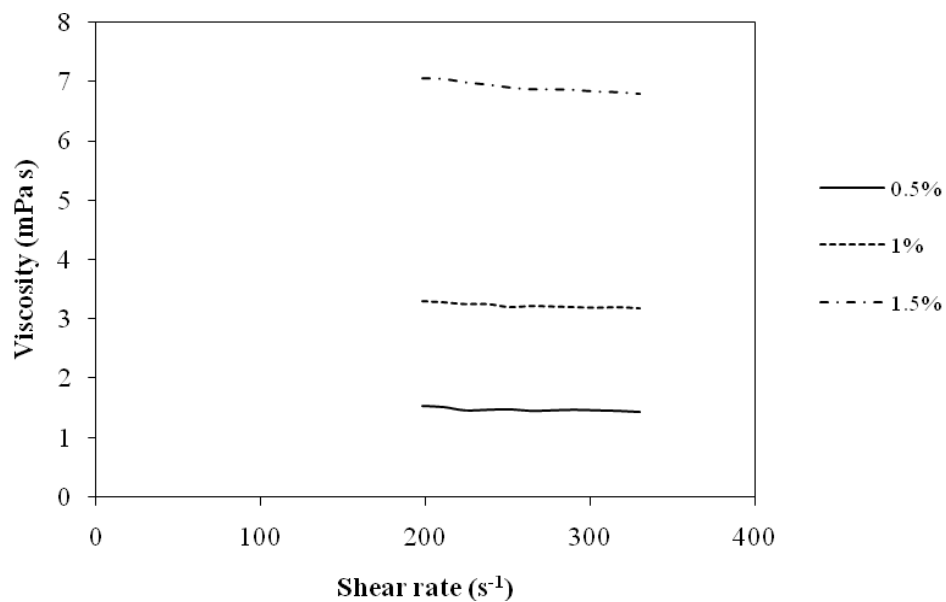


**Figure 4.10** : Viscosities of P(*n*-BA-*co*-MMA) at 1:1 monomer ratio with different chitosan concentrations (MW  $3.7 \times 10^5$  Da).

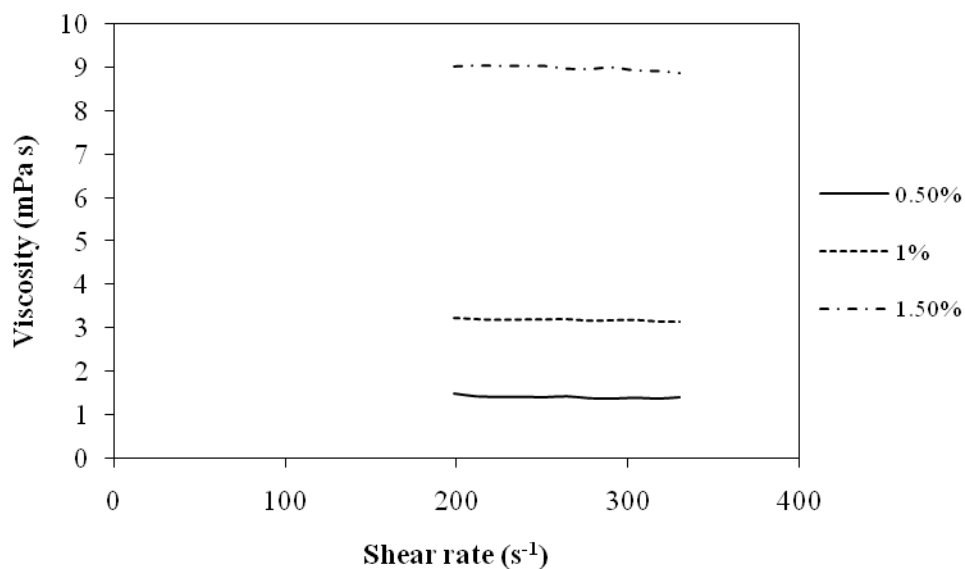


**Figure 4.11** : Viscosities of P(*n*-BA-*co*-MMA) at 1:1 monomer ratio with different chitosan concentration (MW  $8.5 \times 10^5$  Da).

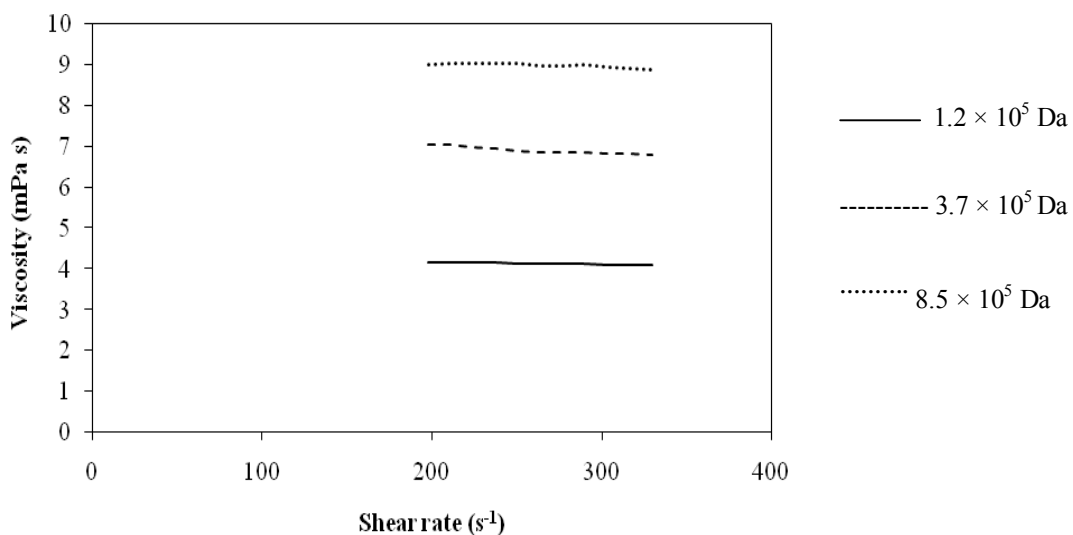


**Figure 4.12** : Viscosities of P(*n*-BA-*co*-MMA) at 1:1 monomer ratio and 1.5%(w/v) with different chitosan molecular weights.

#### 4.5 Characterization of nuclear magnetic resonance

The  $^1\text{H-NMR}$  spectrum of  $\text{P}(n\text{-BA-co-MMA})$  at 1:1 monomer ratio is observed in Figure 4.13. It is reported that in the case of poly(*n*-butyl acrylate), the  $-\text{OCH}_2$  proton appears around  $\delta$  4.0 ppm, and  $\alpha\text{-CH}$ ,  $\beta\text{-CH}_2$ , and  $^4\text{CH}_3$ - protons appear at  $\delta$  2.2-2.4 ppm,  $\delta$  1.8-2.0 ppm, and  $\delta$  0.91-0.96 ppm, respectively. In case of poly(methyl methacrylate), an  $-\text{OCH}_3$  resonance signal appears around  $\delta$  3.5 ppm,  $\beta\text{-CH}_2$ - protons around  $\delta$  2.0 ppm, and  $\alpha\text{-CH}_3$  protons between  $\delta$  1.5 and  $\delta$  1.0 ppm.[16] For the copolymer, the peak between  $\delta$  3.89 and  $\delta$  3.97 ppm is due to  $-\text{OCH}_2$  protons, and at  $\delta$  2.09 ppm due to  $\alpha\text{-CH}$ , at  $\delta$  1.34 ppm due to  $-\text{CH}_2-$ , at  $\delta$  1.56 ppm due to  $-\text{CH}_2-$ , and at  $\delta$  0.91 ppm due to  $-\text{CH}_3$  of *n*-butyl acrylate. The peak obtained at  $\delta$  3.56 ppm corresponds to  $-\text{OCH}_3$  and at  $\delta$  1.11 ppm and  $\delta$  1.23 ppm to  $\alpha\text{-CH}_3$  of methyl methacrylate. The  $\beta\text{-CH}_2$  signal appears at  $\delta$  2.03 and  $\delta$  1.79 ppm. These peak positions are coincided with the results reported for  $\text{P}(n\text{-BA})$  and PMMA. The positions of peak and their intensities suggest that a copolymer of *n*-butyl acrylate and methyl methacrylate has formed in an equimolar proportion. Composition of particle was determined by separation  $\text{P}(n\text{-BA-co-MMA})$  encapsulated with chitosan from homopolymers of  $\text{P}(n\text{-BA})$  and PMMA. It involved a two-step soxhlet extraction: (a) The adsorbed chitosan on the polymer particles was first removed through extraction with 1%v/v acetic acid solution for 16 hours; (b) the purified particles were then extracted with chloroform for 16 hours to separate the chitosan encapsulated copolymer,  $\text{P}(n\text{-BA})$ , and PMMA.  $^1\text{H-NMR}$  spectrum of  $\text{P}(n\text{-BA-co-MMA})$  encapsulated with chitosan at different concentrations (MW  $3.7 \times 10^5$  Da) were observed in a mixture of  $\text{CDCl}_3$  and acetic acid- $d_4$ . Peak at 1.9 ppm suggests the presence of chitin acetyl proton in chitin as shown in Figures 4.14-4.16.

The grafting percentage of chitosan on copolymer main chain is calculated using equation (3). The results show that at 0.5% wt of chitosan concentration (Figures 4.14, 4.17-4.18), the grafting of chitosan increases as the molecular weight increases. (Table 4.6) It indicates that longer polymer chain provides more possibility of grafting reaction due to more grafting sites available. As the concentration of chitosan is enhanced, an increment of the grafting on the particles is attained as well (Table 4.7). Interestingly, the amount of BA present in the copolymer also plays a role in grafting reaction. An increase in BA content results in an increase in chitosan grafting (Table 4.8). The use of chitosan, a cationic polysaccharide derived from chitin, results in a certain grafting percentage (approximately 45-56%). [6] In other words, the chitosan molecules are possibly covalently linked with the copolymers. This result suggests that the amino group of chitosan is chemically bonded to the copolymers. [16] It can be confirmed by the presence of chitin acetyl proton in the copolymers prepared with 1:2, 3:2, and 2:1 monomer ratios as seen in Figures 4.19-4.21.

$$\text{Grafting percentage} = \frac{W_g}{W_t} \times 100 \quad (3)$$

where;  $W_g$  = Weight of the grafted chitosan copolymer  
 $W_t$  = Weight of the soluble polymer

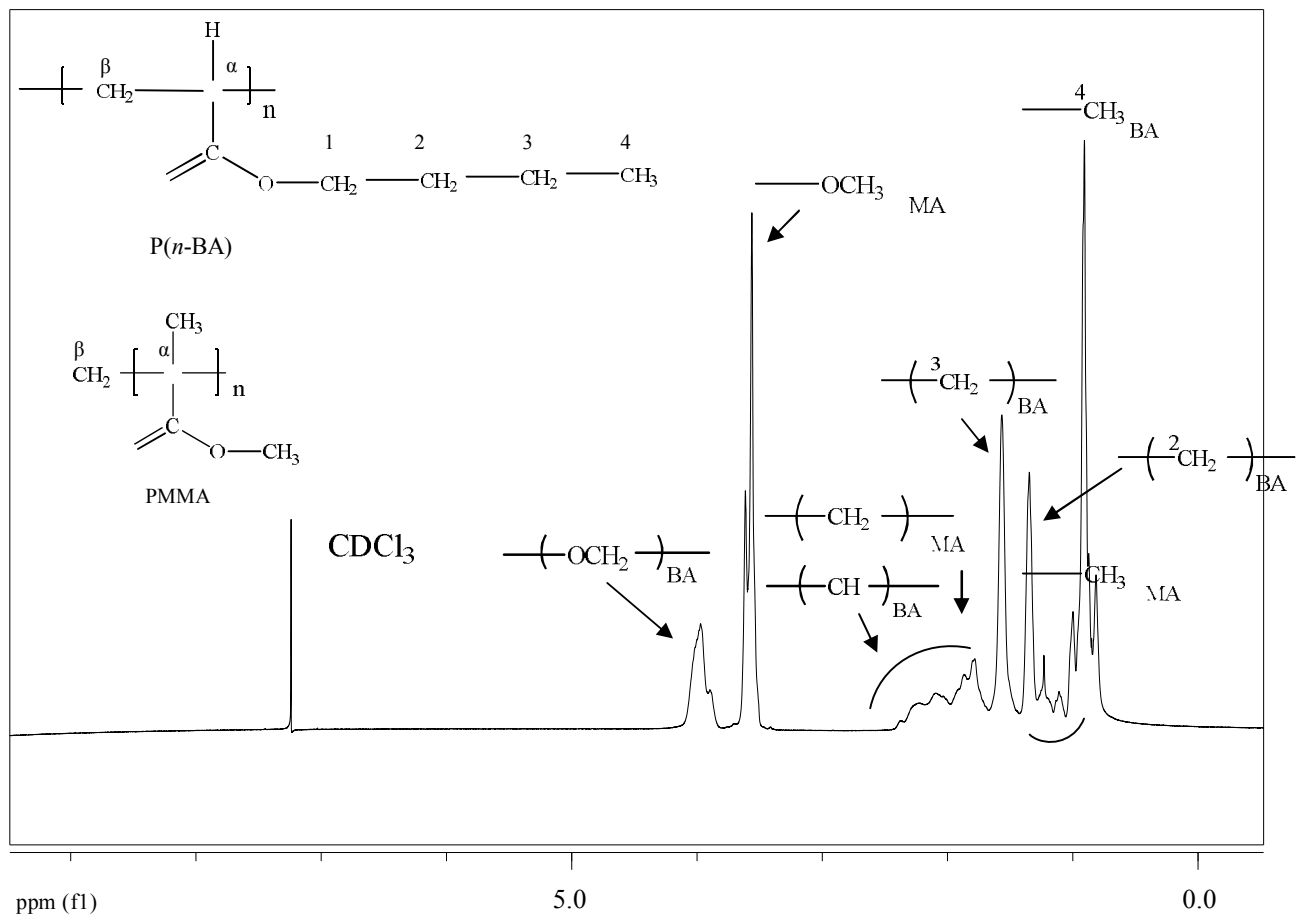


**Figure 4.13 :**  $^1\text{H-NMR}$  spectrum of  $\text{P}(n\text{-BA-co-MMA})$  at 1:1 monomer ratio.

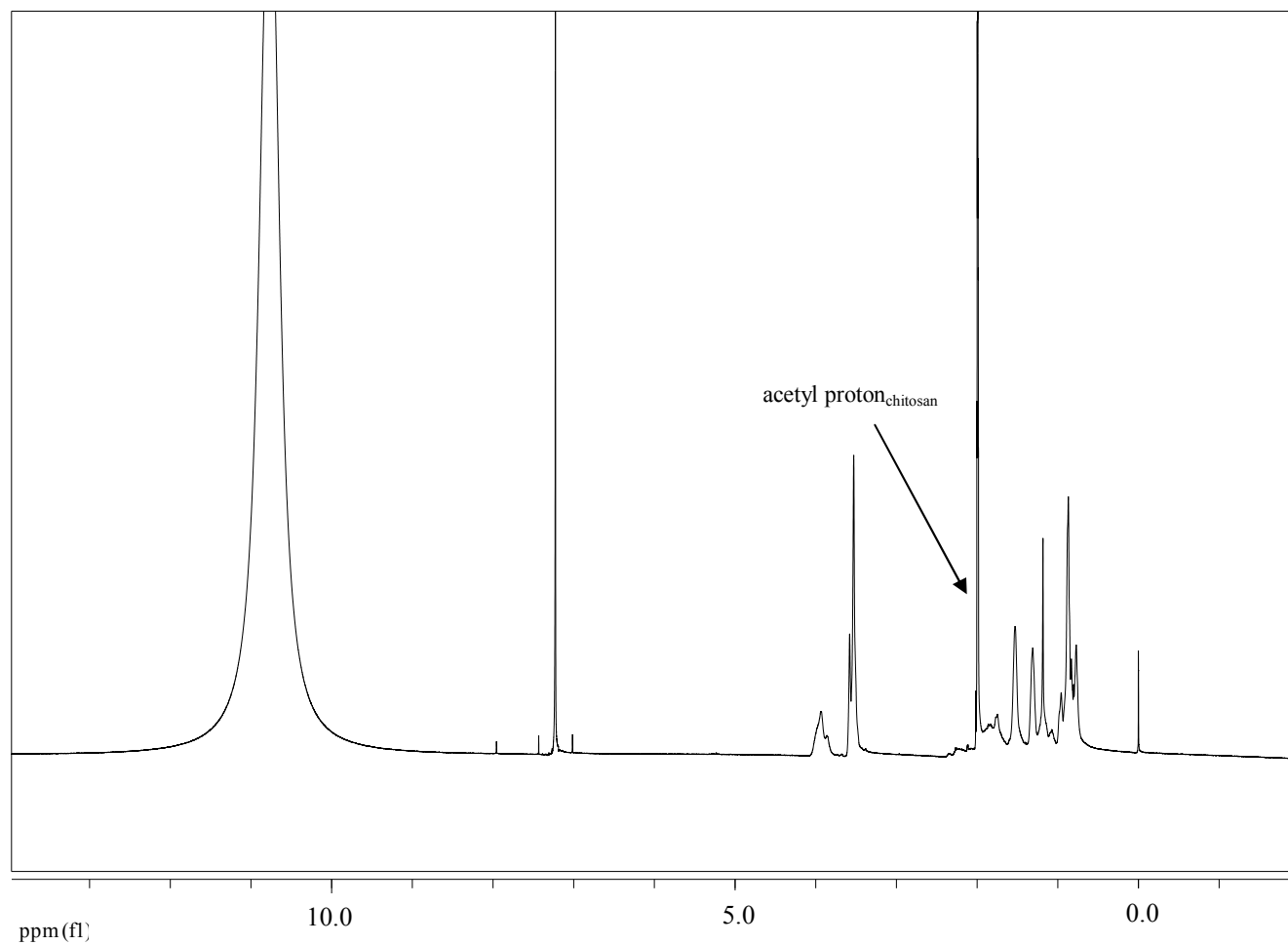


**Figure 4.14 :** <sup>1</sup>H-NMR spectrum of P(*n*-BA-*co*-MMA) at 1:1 monomer ratio encapsulated with chitosan (0.5% w/v, MW  $3.7 \times 10^5$  Da).

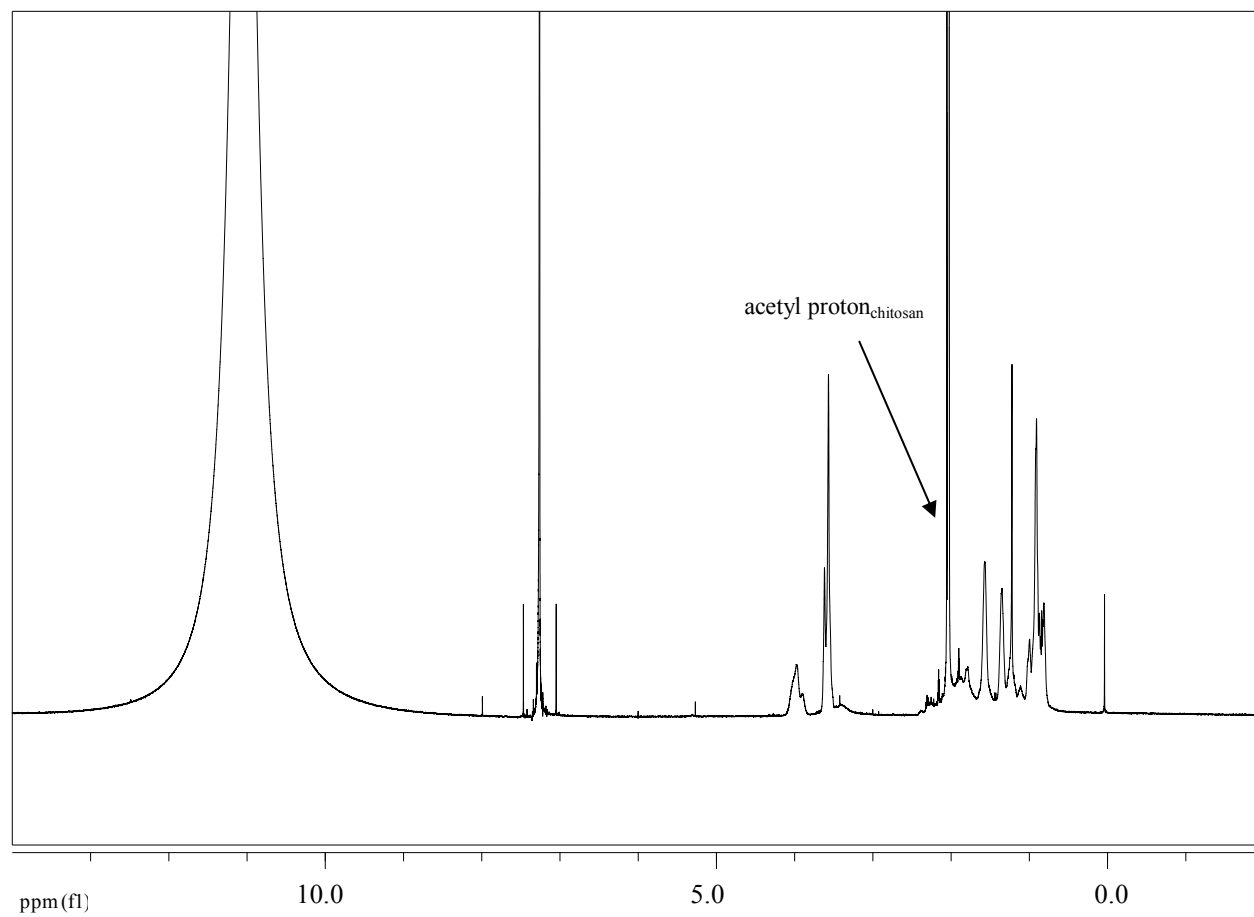


**Figure 4.15 :** <sup>1</sup>H-NMR spectrum of P(*n*-BA-*co*-MMA) at 1:1 monomer ratio encapsulated with chitosan (1% w/v, MW  $3.7 \times 10^5$  Da).

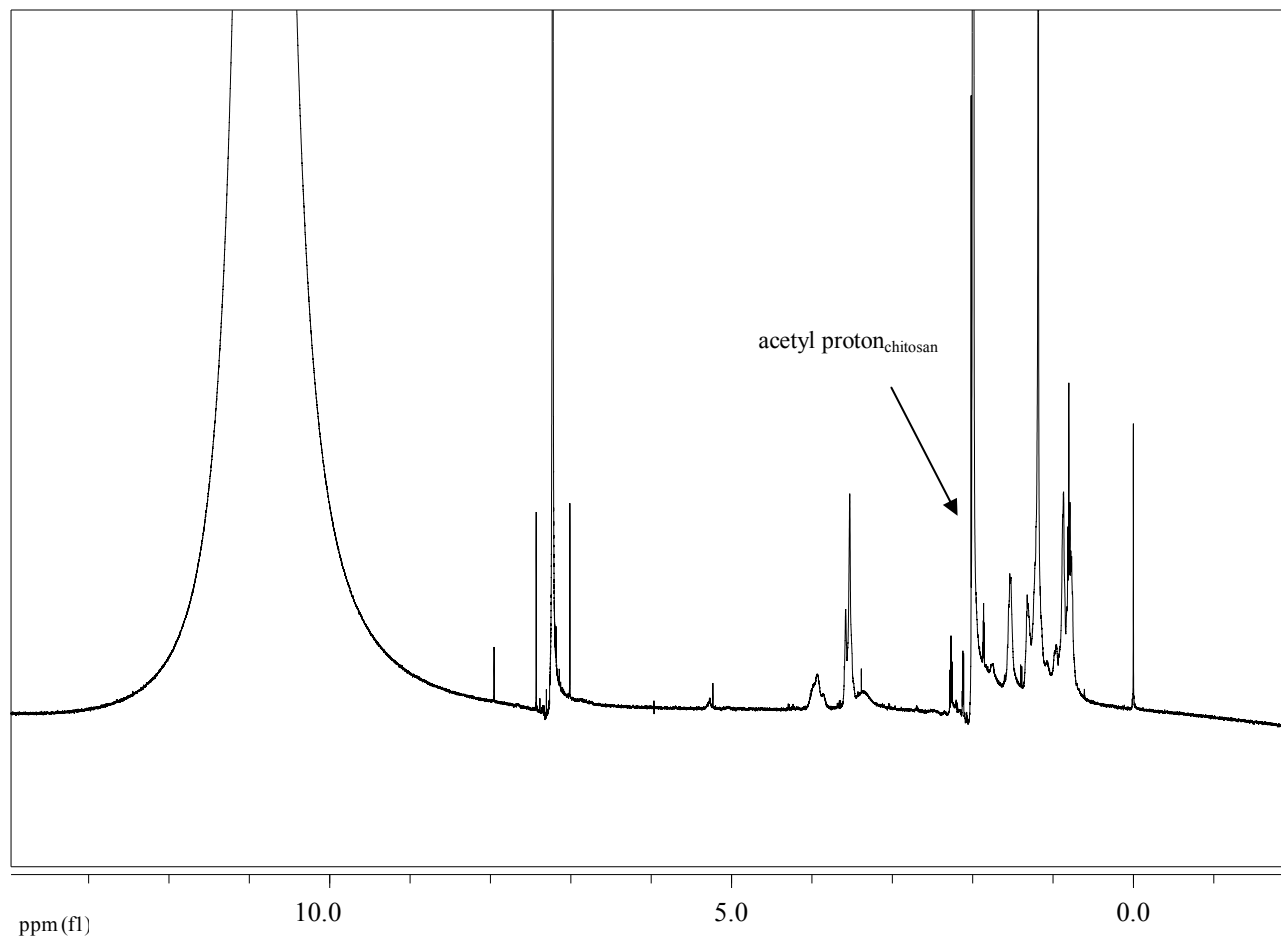


**Figure 4.16 :**  $^1\text{H}$ -NMR spectrum of P(*n*-BA-*co*-MMA) at 1:1 monomer ratio encapsulated with chitosan (1.5% w/v, MW  $3.7 \times 10^5$  Da).

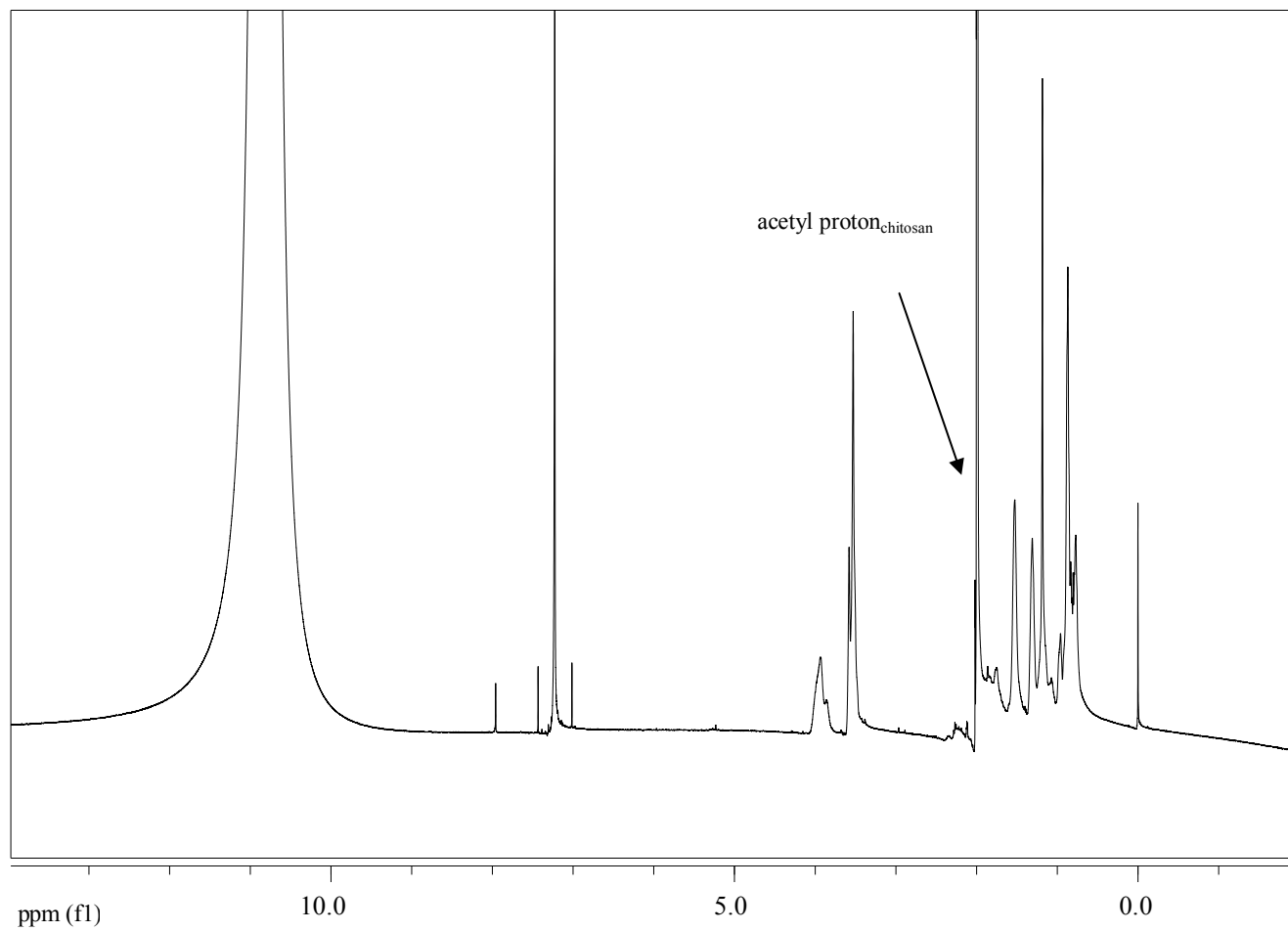


**Figure 4.17 :** <sup>1</sup>H-NMR spectrum of P(*n*-BA-*co*-MMA) at 1:1 monomer ratio encapsulated with chitosan (0.5% w/v, MW  $1.2 \times 10^5$  Da).

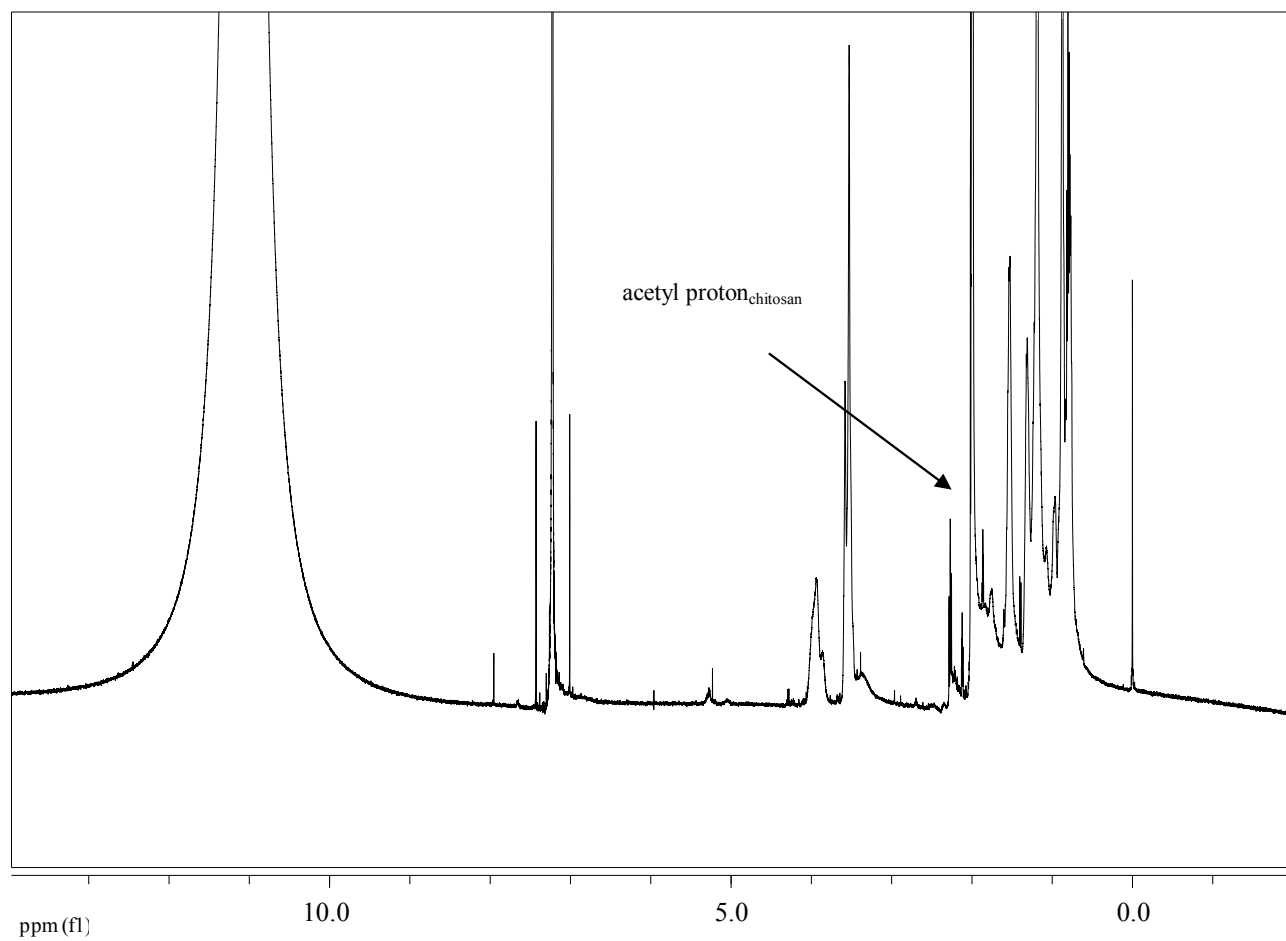


**Figure 4.18 :**  $^1\text{H}$ -NMR spectrum of P(*n*-BA-*co*-MMA) at 1:1 monomer ratio encapsulated with chitosan (0.5% w/v, MW  $8.5 \times 10^5$  Da).

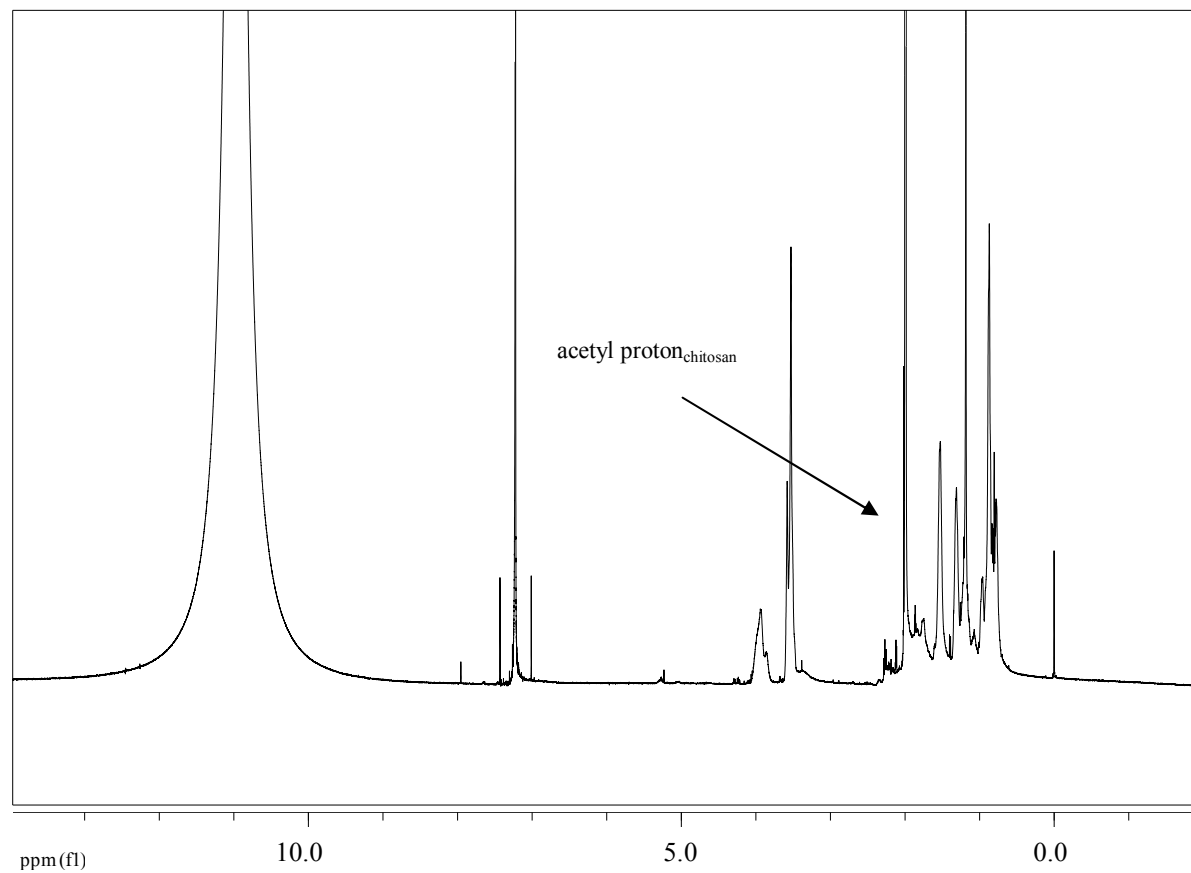


**Figure 4.19 :**  $^1\text{H-NMR}$  spectrum of  $\text{P}(n\text{-BA-co-MMA})$  at 1:2 monomer ratio encapsulated with chitosan (0.5% w/v, MW  $3.7 \times 10^5$  Da).

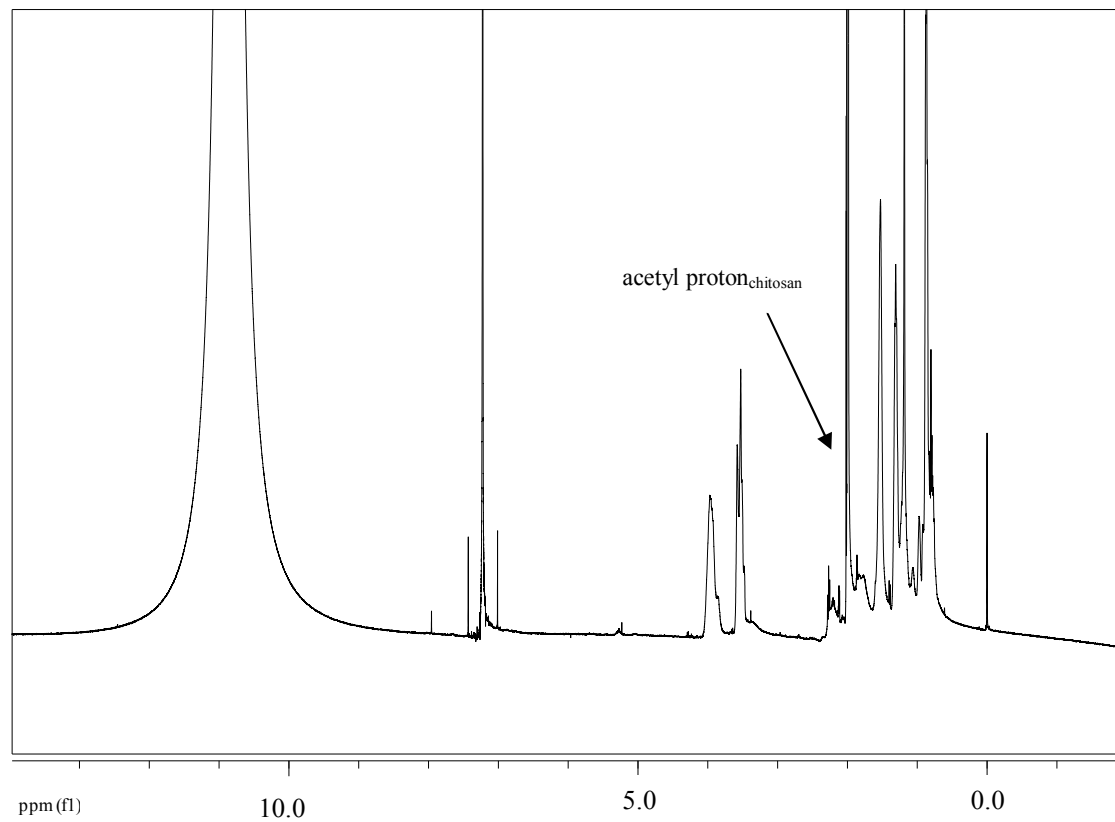


**Figure 4.20 :**  $^1\text{H-NMR}$  spectrum of  $\text{P}(n\text{-BA-co-MMA})$  at 3:2 monomer ratio encapsulated with chitosan (0.5% w/v, MW  $3.7 \times 10^5$  Da).

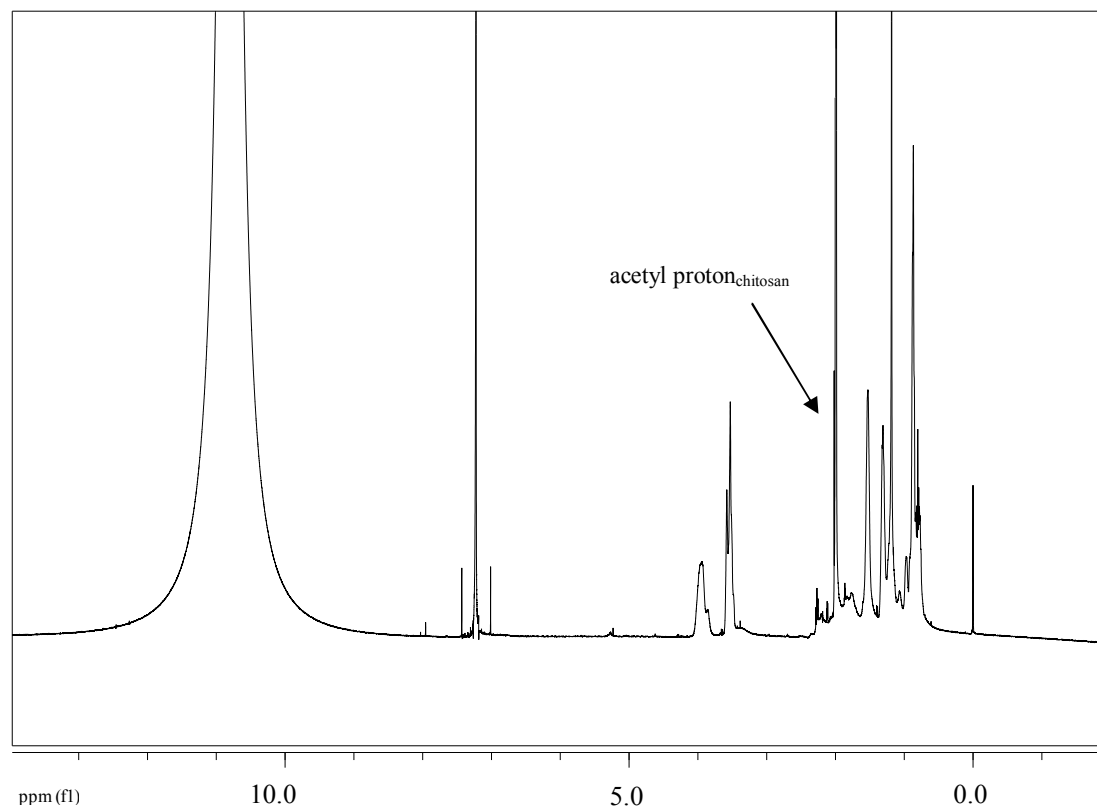


**Figure 4.21** :  $^1\text{H-NMR}$  spectrum of  $\text{P}(n\text{-BA-co-MMA})$  at 2:1 monomer ratio encapsulated with chitosan (0.5% w/v, MW  $3.7 \times 10^5$  Da).

**Table 4.6** Grafting percentage of copolymer (1:1) encapsulated with 0.5% w/v of various molecular weights of chitosan

Polymer	%Grafting
P( <i>n</i> -BA- <i>co</i> -MMA) 1:1/0.5% (MW $1.2 \times 10^5$ Da)	47.7
P( <i>n</i> -BA- <i>co</i> -MMA) 1:1/0.5% (MW $3.7 \times 10^5$ Da)	52.0
P( <i>n</i> -BA- <i>co</i> -MMA) 1:1/0.5% (MW $8.5 \times 10^5$ Da)	52.3

**Table 4.7** Grafting percentage of copolymer (1:1) encapsulated with various chitosan concentrations

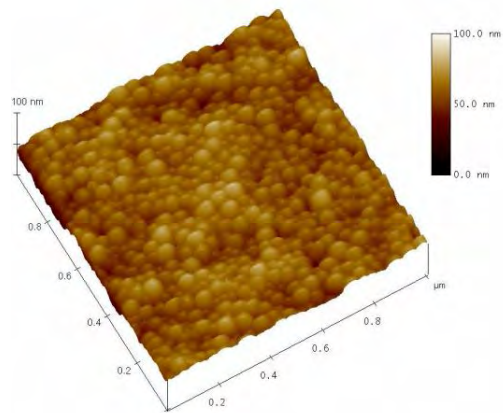
Polymer	%Grafting
P( <i>n</i> -BA- <i>co</i> -MMA) 1:1/0.5% (MW $3.7 \times 10^5$ Da)	52.0
P( <i>n</i> -BA- <i>co</i> -MMA) 1:1/1% (MW $3.7 \times 10^5$ Da)	52.3
P( <i>n</i> -BA- <i>co</i> -MMA) 1:1/1.5% (MW $3.7 \times 10^5$ Da)	54.3

**Table 4.8** Grafting percentage of encapsulated copolymers prepared with various monomer ratios

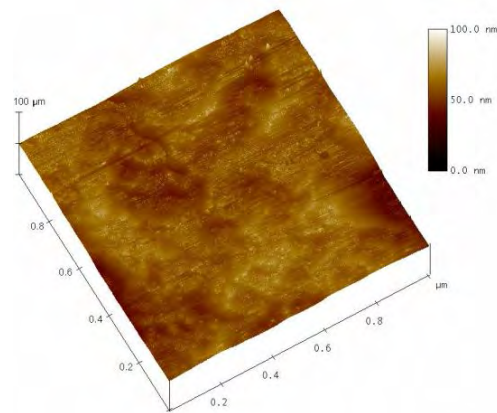
Polymer	%Grafting
P( <i>n</i> -BA- <i>co</i> -MMA) 1:2/0.5% (MW $3.7 \times 10^5$ Da)	44.5
P( <i>n</i> -BA- <i>co</i> -MMA) 1:1/0.5% (MW $3.7 \times 10^5$ Da)	52.0
P( <i>n</i> -BA- <i>co</i> -MMA) 3:2/0.5% (MW $3.7 \times 10^5$ Da)	55.6
P( <i>n</i> -BA- <i>co</i> -MMA) 2:1/0.5% (MW $3.7 \times 10^5$ Da)	54.2

#### 4.6 Atomic Force Microscopy (AFM)

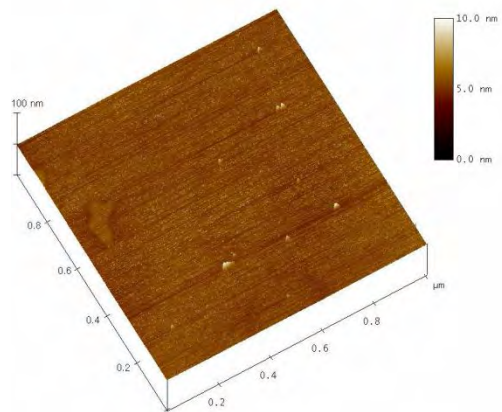
AFM follows statistical analysis to be performed on the scans of the sample surface and provides information on surface roughness. The results are presented in Figure 4.22 for films prepared from P(*n*-BA-*co*-MMA) at different monomer ratios, which dried at room temperature for 7 days. At 1:2 monomer ratio shows incompleting coalescence, since some discrete particles are still visible with a certain degree of deformation. At 1:1, 3:2, and 2:1 monomer ratios, the film formation have gained flatness faster than the film of 1:2 monomer ratio. It can be seen that a decrease in surface roughness is observed when the amount of *n*-BA is increased.



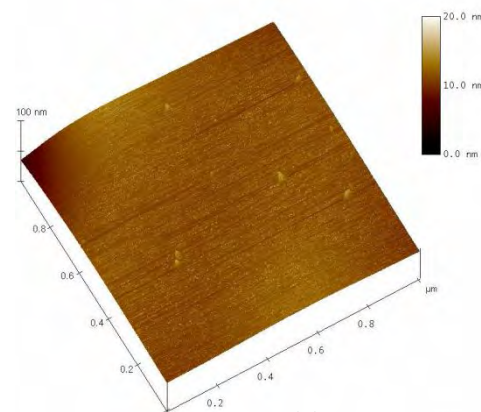
(a)



(b)



(c)



(d)

**Figure 4.22** : AFM images of P(*n*-BA-*co*-MMA) with different monomer ratios (a) 1:2, (b) 1:1, (c) 3:2, (d) 2:1.

Film of copolymer at 1:1 monomer ratio encapsulated with different chitosan concentrations of medium molecular weight is selected to be a representative among other monomer ratios and shown in Figure 4.23. These results indicate that the chitosan encapsulation has an impact on film formation of P(*n*-BA-*co*-MMA). Increasing in the amount of chitosan leads to a pronounced reduction in surface roughness, suggesting that the chitosan encapsulation promotes a smooth film formation. Similarly, an increase in molecular weight of chitosan can affect on film formation in which high molecular weight ( $8.5 \times 10^5$  Da) tends to form a smoother film (Figure 4.24). This is probably due to a rather thick chitosan layer surrounding the copolymers, during film formation, which might have gathered on top surface of the film, influencing on film smoothness (Table 4.9).

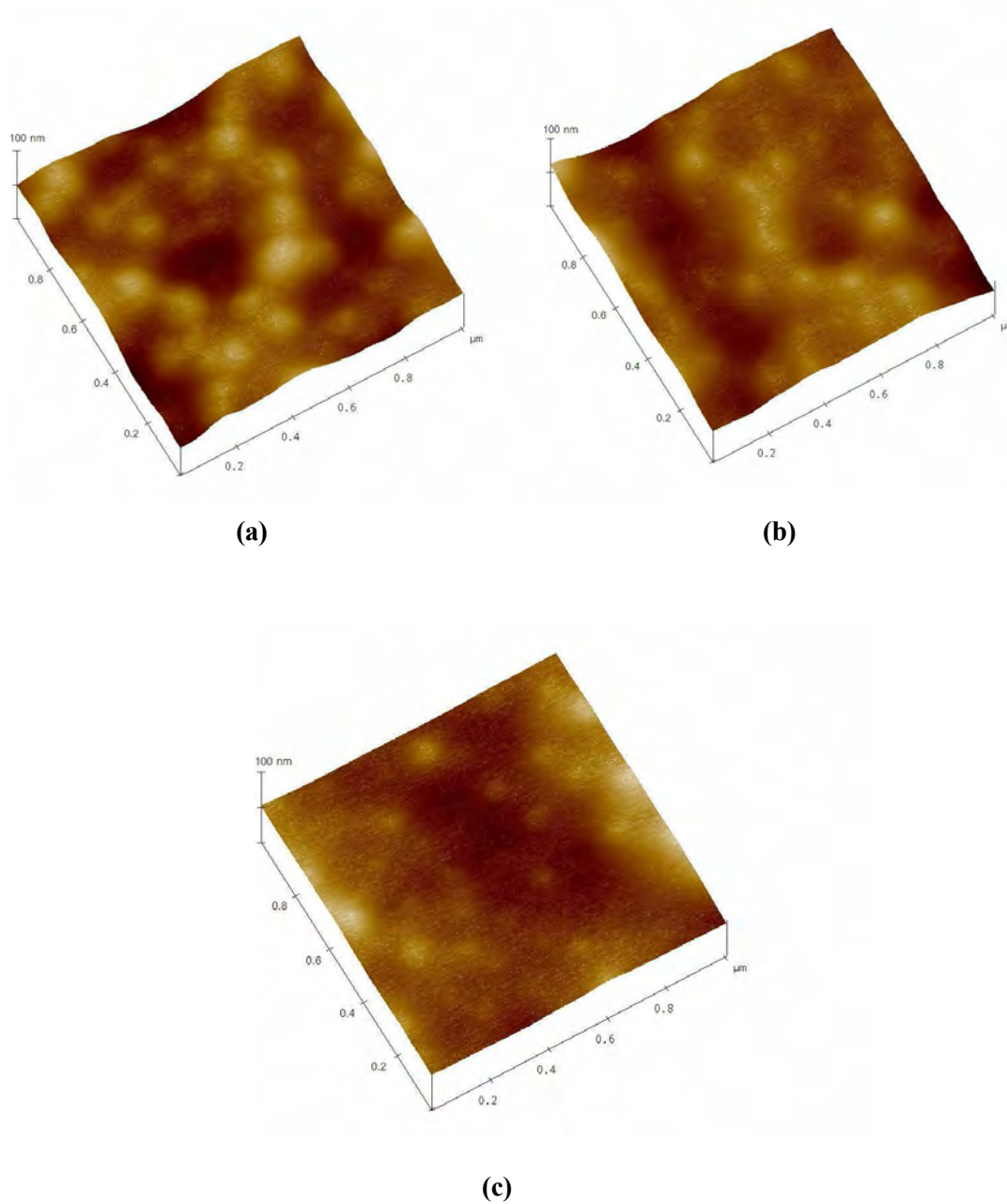


**Figure 4.23** : AFM images of P(*n*-BA-*co*-MMA) at 1:1 monomer ratio encapsulated with different chitosan concentrations ( $3.7 \times 10^5$  Da) (a) 0.5%w/v, (b) 1%w/v, (c) 1.5%w/v.

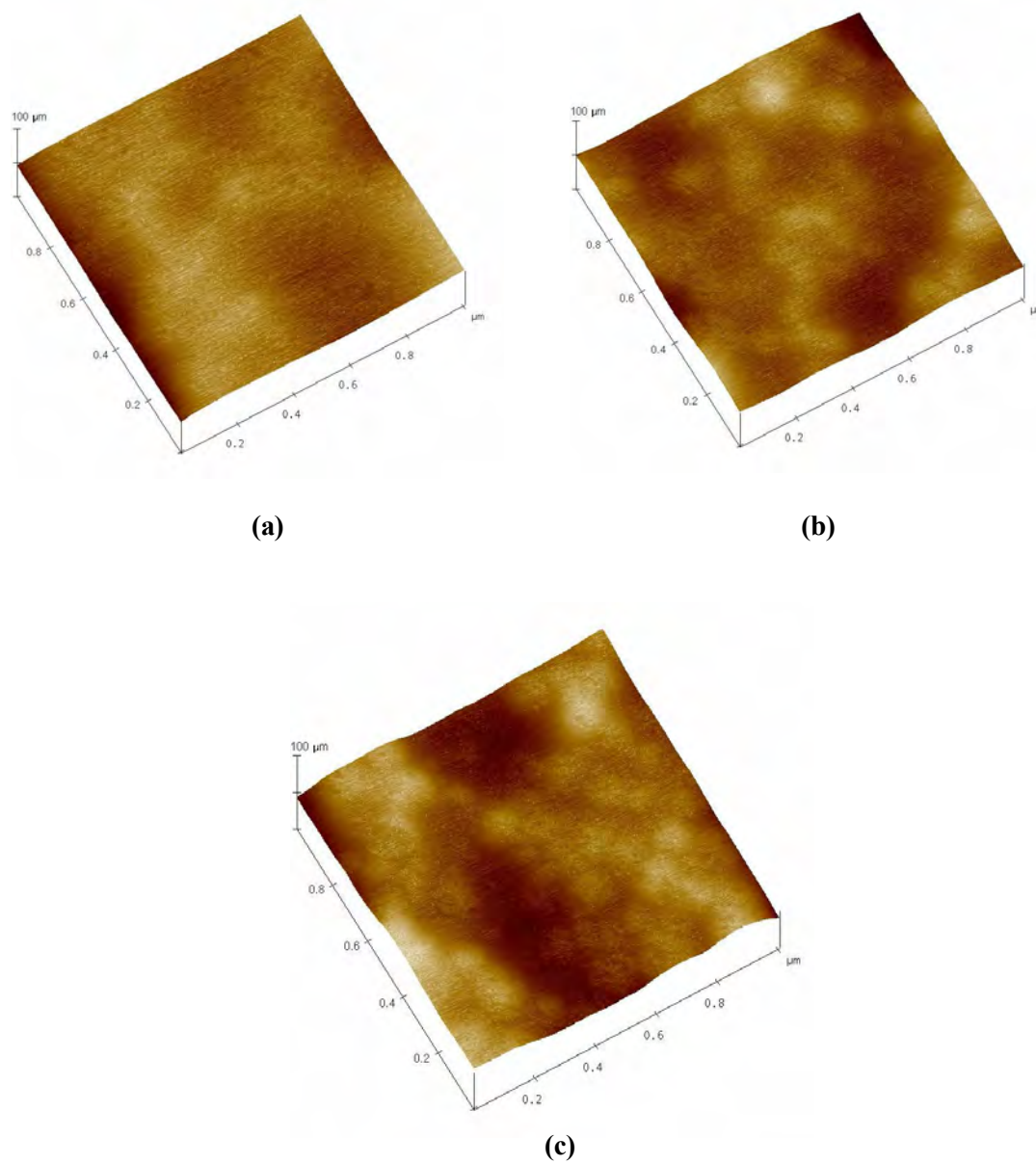


**Figure 4.24** : AFM images of P(*n*-BA-*co*-MMA) at 1:1 monomer ratio encapsulated with different chitosan molecular weights (0.5%w/v) (a)  $1.2 \times 10^5$  Da, (b)  $3.7 \times 10^5$  Da, (c)  $8.5 \times 10^5$  Da.

**Table 4.9** Roughness of P(*n*-BA-*co*-MMA) at 1:1 monomer ratio encapsulated with different chitosan concentrations and molecular weights.

Polymer	Roughness (nm)
P( <i>n</i> -BA- <i>co</i> -MMA) 1:1	0.708
P( <i>n</i> -BA- <i>co</i> -MMA) 1:1/0.5% (MW $1.2 \times 10^5$ Da)	18.405
P( <i>n</i> -BA- <i>co</i> -MMA) 1:1/1% (MW $1.2 \times 10^5$ Da)	6.245
P( <i>n</i> -BA- <i>co</i> -MMA) 1:1/1.5% (MW $1.2 \times 10^5$ Da)	4.270
P( <i>n</i> -BA- <i>co</i> -MMA) 1:1/0.5% (MW $3.7 \times 10^5$ Da)	8.065
P( <i>n</i> -BA- <i>co</i> -MMA) 1:1/1% (MW $3.7 \times 10^5$ Da)	6.660
P( <i>n</i> -BA- <i>co</i> -MMA) 1:1/1.5% (MW $3.7 \times 10^5$ Da)	3.212
P( <i>n</i> -BA- <i>co</i> -MMA) 1:1/0.5% (MW $8.5 \times 10^5$ Da)	7.408
P( <i>n</i> -BA- <i>co</i> -MMA) 1:1/1% (MW $8.5 \times 10^5$ Da)	5.621
P( <i>n</i> -BA- <i>co</i> -MMA) 1:1/1.5% (MW $8.5 \times 10^5$ Da)	3.458

#### 4.7 Bending Test

The sample preparation was done by pouring the amount of 17 g of latex into an acrylic mold filled with aluminium sheet and ovened at 80°C for 3-4 hours. The coating material under test was applied at uniform thickness to a sheet metal as described in ASTM D522-93a. The procedure of testing is as follows: place the test panel over a mandrel with the uncoated side in contact and with at least 2 inch overhang on either side. Using a steady pressure of the fingers, bend the panel approximately 180° around the mandrel at a uniform velocity in a time of 1 second unless an alternative time is agreed upon between the panel immediately for cracking visible to the unaided eye. If cracking has not occurred, repeat the procedure using successively smaller diameter mandrels on previously untested areas of specimen until failure occurs or until the smallest diameter mandrel has been used. It is observed that the monomer ratio dominates on film property, specially at 1:2, which contains the highest amount of MMA, resulting in a brittle coating. Typically, film property of PMMA can be brittle when it is formed at room temperature. In contrast, film coatings prepared with other monomer ratios which contain high amount of BA yield good flexibility of film. With chitosan encapsulation, the film still remains good flexibility or unchanged.

**Table 4.10** Effect of chitosan concentration and molecular weight of P(*n*-BA-co-MMA) on the bending test

Polymer	monomer ratio			
	1:2	1:1	3:2	2:1
no chitosan	cracked	un-cracked	un-cracked	un-cracked
0.5%, MW $1.2 \times 10^5$ Da	cracked	un-cracked	un-cracked	un-cracked
1%, MW $1.2 \times 10^5$ Da	cracked	un-cracked	un-cracked	un-cracked
1.5%, MW $1.2 \times 10^5$ Da	cracked	un-cracked	un-cracked	un-cracked
0.5%, MW $3.7 \times 10^5$ Da	cracked	un-cracked	un-cracked	un-cracked
1%, MW $3.7 \times 10^5$ Da	cracked	un-cracked	un-cracked	un-cracked
1.5%, MW $3.7 \times 10^5$ Da	cracked	un-cracked	un-cracked	un-cracked
0.5%, MW $8.5 \times 10^5$ Da	cracked	un-cracked	un-cracked	un-cracked
1%, MW $8.5 \times 10^5$ Da	cracked	un-cracked	un-cracked	un-cracked
1.5%, MW $8.5 \times 10^5$ Da	cracked	un-cracked	un-cracked	un-cracked

#### 4.8 Differential scanning calorimetry

The results of DSC thermograms of P(*n*-BA-*co*-MMA) with different monomer ratios are given in Figure 4.25, suggesting that the glass transition temperatures ( $T_g$ ) of the synthesized copolymers are corresponded to the monomer ratio. From the figure, the copolymers with the ratios of BA to MMA at 1:1 and 1:2 exhibit  $T_g$  at 37°C and 53°C, respectively. These  $T_g$ s are in between the  $T_g$ s of PBA homopolymer (-47°C) and PMMA homopolymer (105°C), suggesting the copolymer structure. However, at 3:2 and 2:1 monomer ratios, the  $T_g$ s cannot be detected. Since they might have been out of range of investigated temperature. It is reported that the  $T_g$ s of copolymers synthesized at 3:2 and 2:1 (BA:MMA) are founded at 4°C and -8.3°C, respectively. [17],[14] Figure 4.26 shows the transition detected in the thermogram of chitosan film. A first endothermic peak is observed at 140°C, which attributed to the evaporation of absorbed water in the inner chitosan structure. A second effect is observed between 150-180°C with an exothermic peak at 174°C. This effect is also associated to a mass loss which corresponded to the thermal degradation of polymeric chain with vaporization of volatile compounds. The pyrolysis of polysaccharide structure starts by a random split of the glycosidic bonds, followed by a further decomposition forming acetic acid. For P(*n*-BA-*co*-MMA) prepared at 1:1 monomer ratio encapsulated with chitosan, however, the  $T_g$  of copolymers cannot be observed but the exothermic peak of chitosan can be seen between 210-230°C, which corresponds to the thermal property of chitosan. The observed lower enthalpy ( $\Delta H$ ) value for the decomposition of chitin suggests that the decomposition efficiency could

be different from its N-deacetylated analogues, because of difference in the mechanism of cleavage of N-acetyl groups (Figure 4.27).[18]

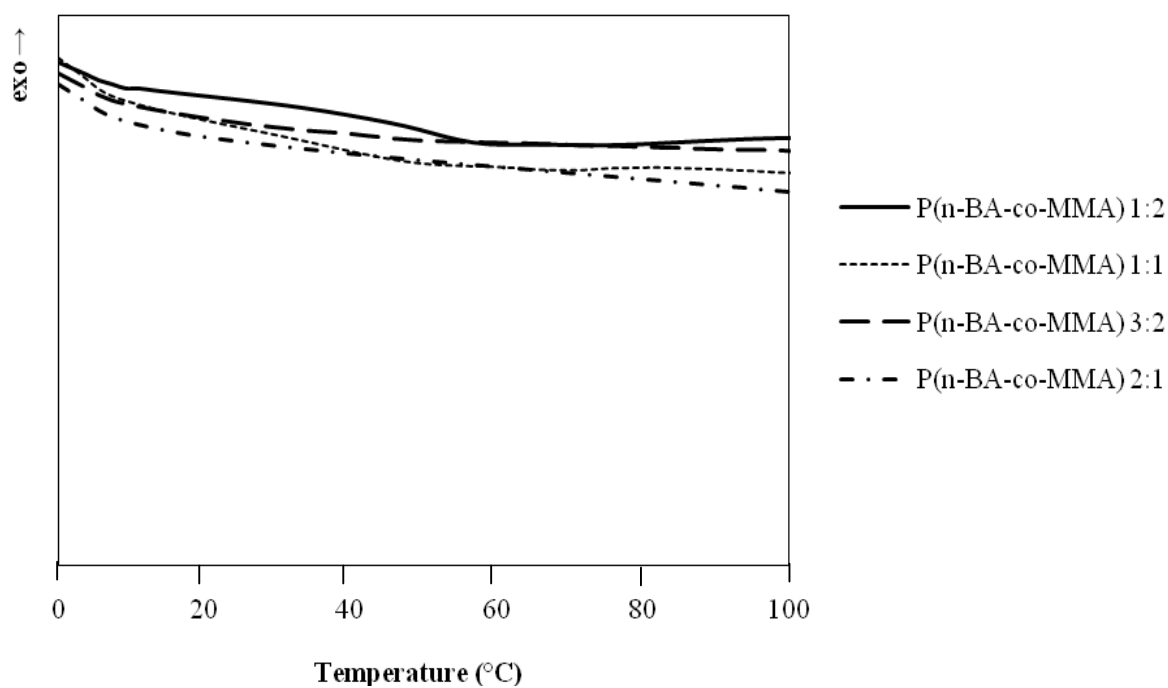


**Figure : 4.25** DSC thermograms of P(*n*-BA-*co*-MMA) prepared with different monomer ratios.

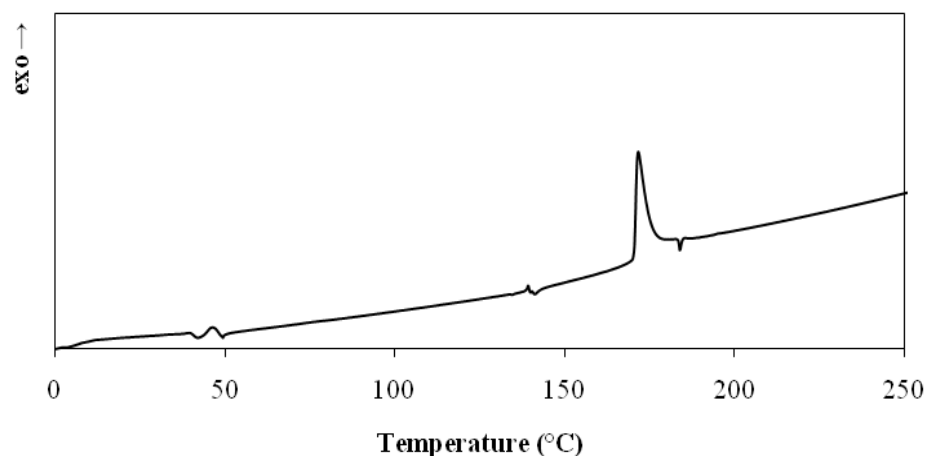


**Figure 4.26** : DSC thermogram of chitosan at 1%w/v (MW  $3.7 \times 10^5$  Da).

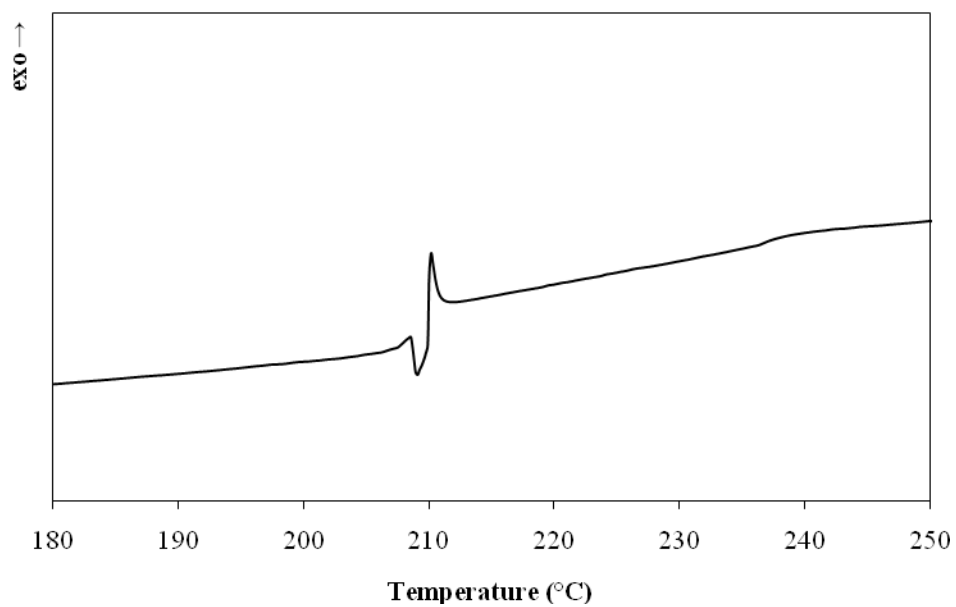


**Figure 4.27** : DSC thermogram of P(*n*-BA-co-MMA) at 1:1 monomer ratio encapsulated with chitosan (1%w/v, MW  $3.7 \times 10^5$  Da).

## CHAPTER V

### CONCLUSION

#### 5.1 Conclusion

The effect of monomer ratio, molecular weight and concentration of chitosan on colloidal and film properties of the copolymer particles was investigated. The result showed that the percentage of monomer conversion was achieved at high conversion (approximately 85-90%). P(*n*-BA-*co*-MMA) encapsulated with chitosan prepared at different monomer ratios and molecular weights and concentrations of chitosan.

TEM micrographs of the copolymer particles and the copolymer particles encapsulated with chitosan showed that the particles obtained were spherical. The chitosan layer seemed to gain more thickness according to the molecular weight and concentration of chitosan.

The particle sizes prepared with various monomer ratios were in proximity and rather small (in the range of 55-65 nm), while the average size chitosan encapsulated copolymer particles were larger (144-624.6 nm). As the concentrations and molecular weights of chitosan were increased, the particles were enlarged according to the chitosan encapsulation layer. Measurement of surface charge of the copolymer encapsulated with chitosan indicated that the positive charge was present on the particle surface when the chitosan was added because the amino groups (NH<sub>2</sub>) in the chitosan became cationic NH<sub>3</sub><sup>+</sup> groups in the acidic solution. The encapsulated particle size tended to decrease as the amount of BA was increased.

The chemical structure of the copolymer particles encapsulated with chitosan was characterized by  $^1\text{H-NMR}$  in which % grafting of copolymers depended on the concentrations and molecular weights of chitosan. It indicated that longer polymer chain provides more possibility of grafting reaction due to more grafting sites available.

The viscosities of  $\text{P}(n\text{-BA-co-MMA})$  emulsions were decreased with increasing the contents of  $n\text{-BA}$  in the monomer feed. They appeared in close proximity, corresponding to the similarity in the particle size. When the particles were encapsulated, the viscosity of the emulsion was also enhanced. The effect was more pronounced at 1% wt and 1.5% wt of chitosan.

As chitosan concentration was increased, the AFM micrographs exhibited that the roughness of copolymers was decreased. At 1:1, 3:2, and 2:1 monomer ratios, the film formation gained flatness faster than the film of 1:2 monomer ratio. It can be seen that a decrease in surface roughness was observed when the amount of  $n\text{-BA}$  was increased.

The result of bending test revealed the flexibility of the coating obtained from the encapsulated particles. Film coatings prepared with the copolymers containing high amount of BA yielded good flexibility. With chitosan encapsulation, the films still remained good flexibility or unchanged, suggesting that having chitosan encapsulation layer helped promoting good film formation.

## REFERENCES

- [1] Lovell P.A., El-Aasser M.S. Emulsion Polymerization and Emulsion Polymers Chichester : John Wiley and Sons, (1997) 38.
- [2] Herk A.V. Chemistry and Technology of Emulsion Polymerisation. Oxford : Blackwell Publisher, (2005) 60-72.
- [3] Lertsutthiwong P., How N.G., Chandkrachang S., Stevens W.F. Effect of chemical treatment on the characteristics of shrimp chitosan. Journal of Metals, Materials and Minerals 12 (2002) 11-18.
- [4] Ye W., Leung M.F., Xin J., Kwong T.L., Lee D.K.L., and Li P. Novel core-shell particles with poly(n-butyl acrylate) cores and chitosan shells as an antibacterial coating for textiles. Polymer 46 (2005) 10538-10543.
- [5] Mun S., Decker E.A., and McClements D.J. Influence of droplet characteristics on the formation of oil-in-water emulsions stabilized by surfactant-chitosan layers. Langmuir 21(14) (2005) 6228-6234.
- [6] Nilsson K. Film formation of latex in dry coating film. Master's Thesis, Department of Chemical Engineering, Graduate School, Karlstads University, 2007.
- [7] Li P., Zhu J.M., Sunintaboon P., and Harris F.W. New route to amphiphilic core-shell polymer nanospheres: Graft copolymerization of methyl methacrylate from water-soluble polymer chains containing amino groups. Langmuir 18(22) (2002) 8641-8646.
- [8] Tiğli R.S., Evren V. Synthesis and characterization of pure poly(acrylate)

latexes. Progress in Organic Coating 52 (2005) 144-150.

- [9] Xue C.H., Shi M.M., Chen H.Z., Wu G., Wang M. Preparation and application of nanoscale microemulsion as binder for fabric inkjet printing. Colloids and Surfaces A: Physicochemical and Engineering Aspects 287 (2006) 147-152.
- [10] Nunes J.S., Vasconcelos C.L., Dantas T.N.C., Pereira M.R., Fonseca J.L.C. Electrokinetic behavior of a poly(butyl acrylate-co-methacrylic acid) latex. Colloids and Surfaces A: Physicochemical and Engineering Aspects 275 (2005) 148-152.
- [11] Ogawa S., Decker E.A., McClements D.J. Production and characterization of o/w emulsions containing cationic droplet stabilized by lecithin-chitosan membranes. Journal of Agricultural and Food Chemistry 51 (2003) 2806-2812.
- [12] Mun S., Decker E.A., McClements D.J. Effect of molecular weight and degree of deacetylation of chitosan on the formation of oil-in-water emulsions stabilized by surfactant-chitosan membranes. Journal of Colloid and Interface Science 296 (2006) 581-590.
- [13] Kim D.G., Jeong Y.I., Choi C., Roh S.H., Kang S.K., Jang M.K., Nah J.W. Retinol-encapsulated low molecular water-soluble chitosan nanoparticles. International Journal of Pharmaceutics 319 (2006) 130-138.
- [14] Zhang M.G., Weng Z.X., Huang Z.M., Pan Z.R. Effects of monomer polarity on MMA/BA/NaMA emulsifier-free emulsion

- copolymerization. European Polymer Journal 34 (1997) 1243-1247.
- [15] P. Li, Zhu J., Sunintaboon P., Harris F.W. Preparation of latexes with poly(methyl methacrylate) cores and hydrophilic polymer shell containing amino groups. Journal of Dispersion Science and Technology 24 (2003) 607-613.
- [16] Roy S., Devi S. High solids contents semicontinuous microemulsion copolymerization of methylmethacrylate and butyl acrylate. Polymer 38 (1996) 3325-3331.
- [17] Liu Y., Haley J.C., Deng K., Lau W., Winnik M.A. Effect of polymer composition on polymer diffusion in poly(butyl acrylate-co-methyl methacrylate) latex film. Macromolecules 40 (2007) 6422-6431.
- [18] López F.A., Mercê A.L.R., Alguacil F.J., Delgado A.L. A kinetic study of the thermal behaviour of chitosan. Journal of Thermal Analysis and Calorimetry 91 (2008) 633-639.

## **APPENDICES**

## APPENDIX A

### VISCOSITY OF COPOLYMERS

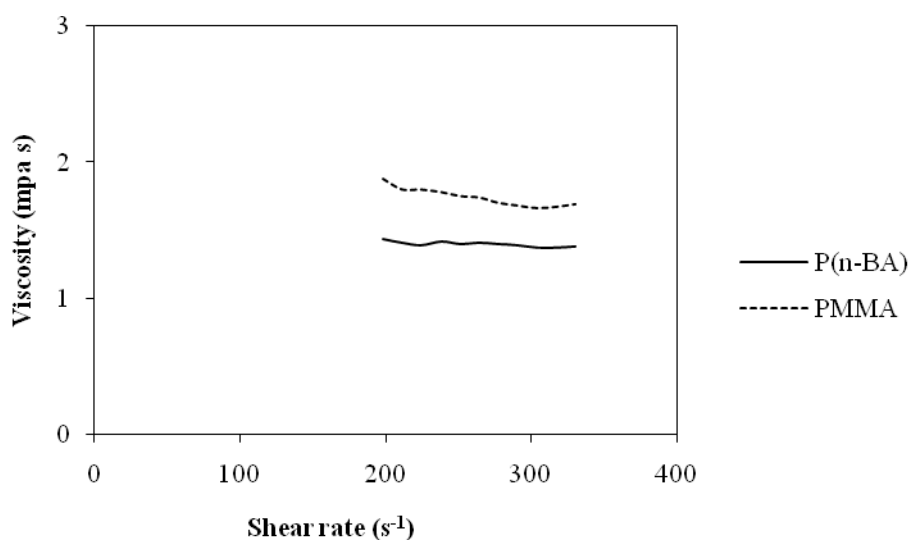


**Figure A.1** : Viscosities of P(*n*-BA) and PMMA.

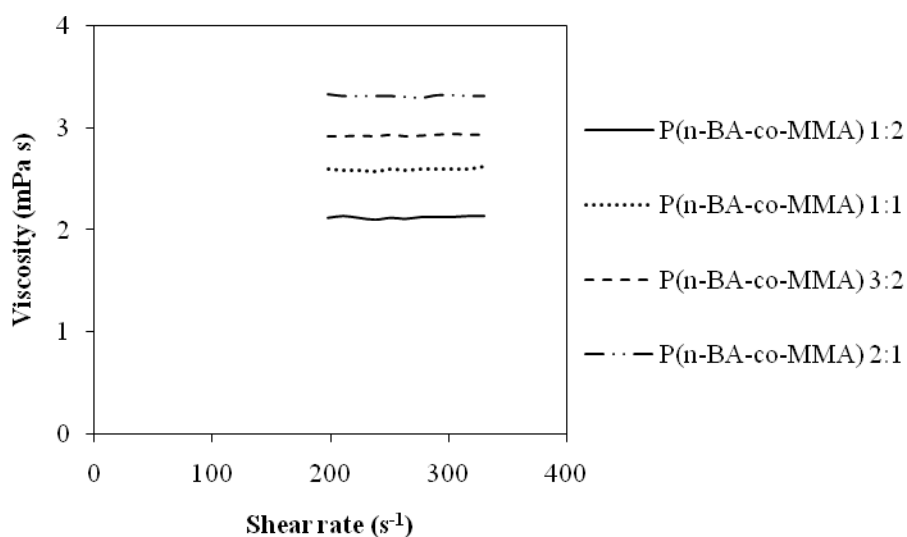


**Figure A.2** : Viscosities of P(*n*-BA-co-MMA) with different monomer ratios and 1%(w/v) chitosan concentration (MW  $1.2 \times 10^5$  Da).

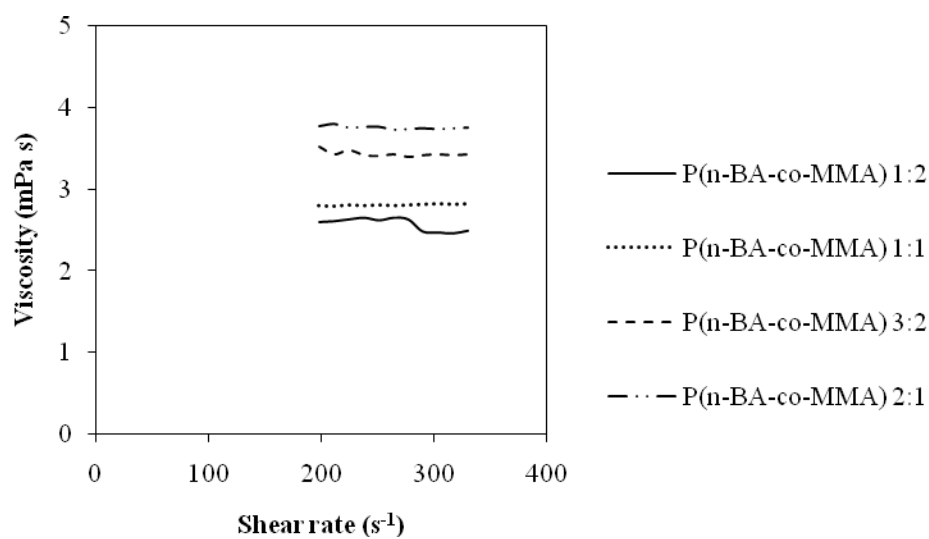


**Figure A.3** : Viscosities of P(*n*-BA-*co*-MMA) with different monomer ratios and 1%(w/v) chitosan concentration (MW  $3.7 \times 10^5$  Da).

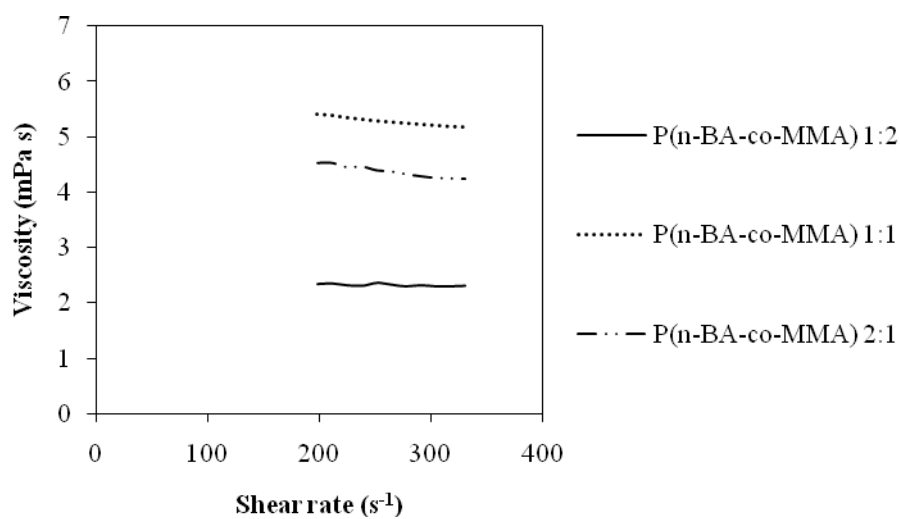
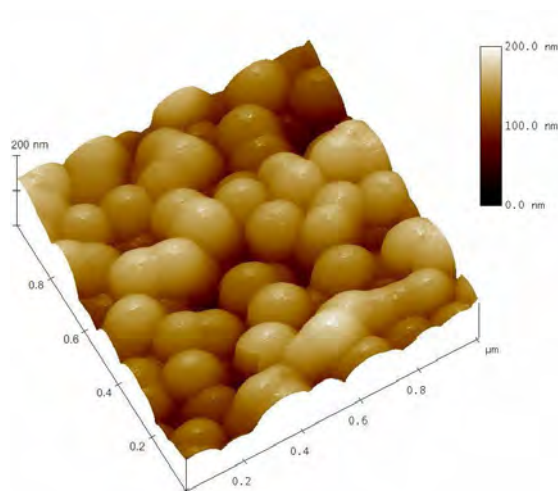


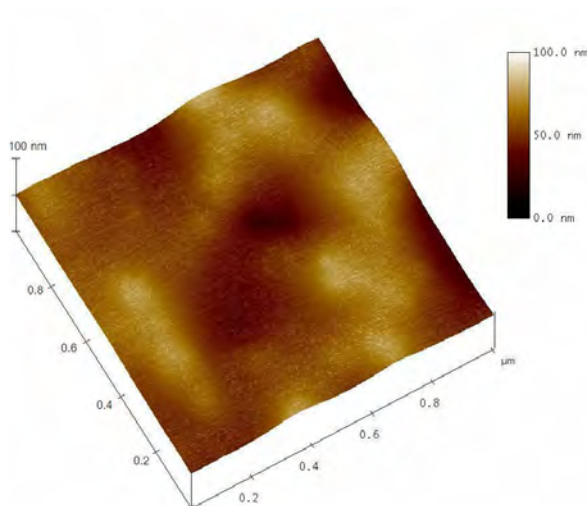
**Figure A.4** : Viscosities of P(*n*-BA-*co*-MMA) with different monomer ratios at 1%(w/v) chitosan concentration (MW  $8.5 \times 10^5$  Da).

## APPENDIX B

### AFM IMAGES



(a)



(b)

**Figure B.1** : AFM images of P(*n*-BA-*co*-MMA) with different monomer ratios encapsulated with chitosan (0.5% w/v, MW  $1.2 \times 10^5$  Da) (a) P(*n*-BA-*co*-MMA) 1:2, (b) P(*n*-BA-*co*-MMA) 3:2.

## APPENDIX C

## DSC THERMOGRAMS

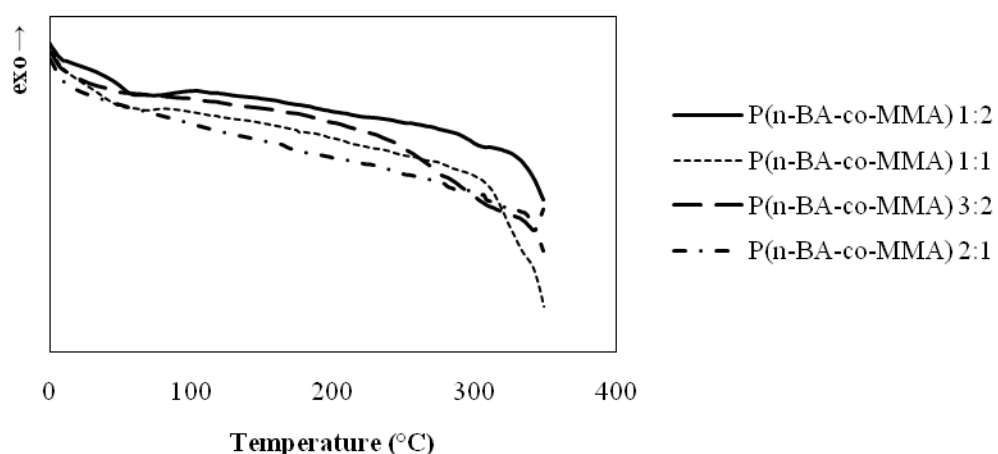


**Figure C.1** : DSC thermograms of P(*n*-BA-*co*-MMA) prepared with different monomer ratios.

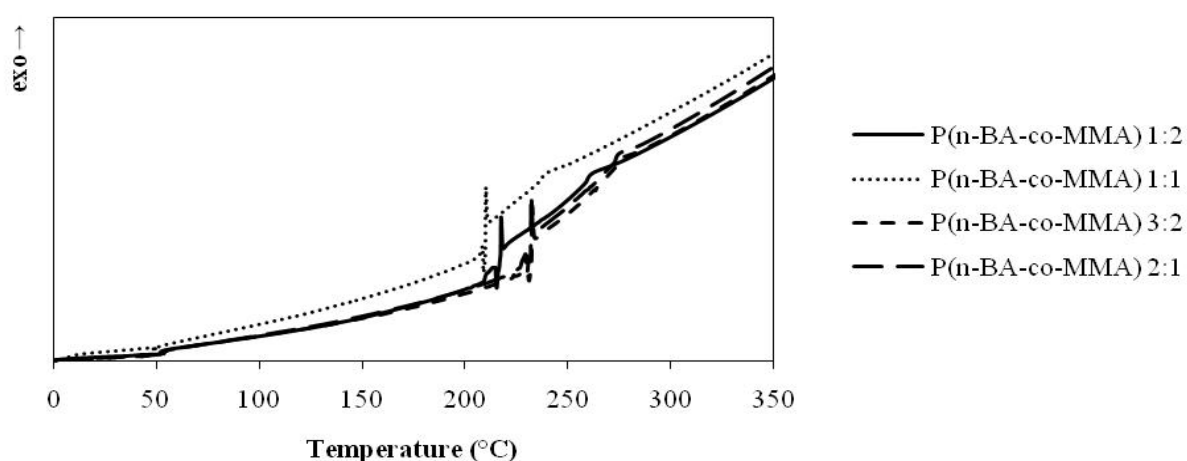


**Figure C.2** : DSC thermograms of P(*n*-BA-*co*-MMA) prepared at various monomer ratios encapsulated with 1%w/v, MW  $3.7 \times 10^5$  Da.

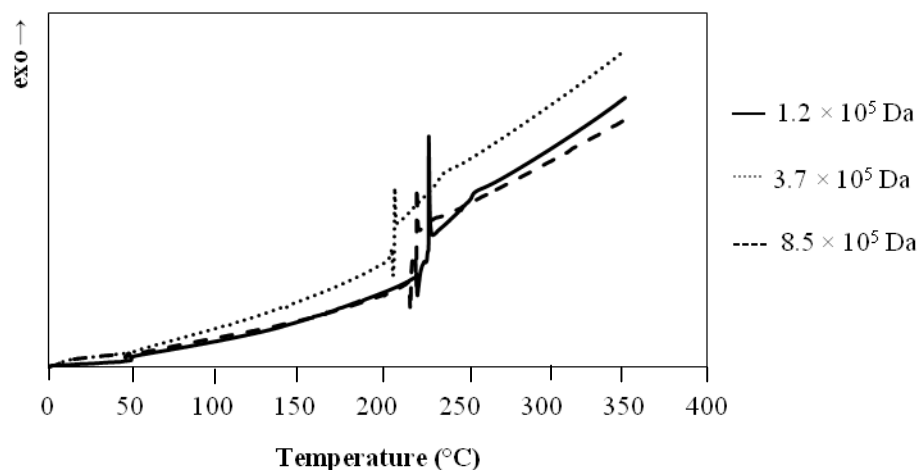


**Figure C.3** : DSC thermograms of P(*n*-BA-*co*-MMA) at 1:1 monomer ratio encapsulated with different molecular weights of chitosan (1%w/v).

**APPENDIX D**  
**SURFACE TENSION**

**Table D.1** Surface tension of copolymers with different monomer ratios

Polymer	Surface tension (mN/m)
PMMA	54.6
P( <i>n</i> -BA)	49.4
P( <i>n</i> -BA- <i>co</i> -MMA) 1:2	52.4
P( <i>n</i> -BA- <i>co</i> -MMA) 1:1	53.8
P( <i>n</i> -BA- <i>co</i> -MMA) 3:2	53.4
P( <i>n</i> -BA- <i>co</i> -MMA) 2:1	53.1

**Table D.2** Surface tension of encapsulated chitosan copolymers with different molecular weights (0.5%w/v)

Polymer	surface tension (mN/m)		
	0.5% w/v		
	$1.2 \times 10^5$ Da	$3.7 \times 10^5$ Da	$8.5 \times 10^5$ Da
P( <i>n</i> -BA- <i>co</i> -MMA) 1:1	$62.8 \pm 0.7$	$55.1 \pm 0.9$	$58.6 \pm 1.7$
P( <i>n</i> -BA- <i>co</i> -MMA) 1:2	$61.5 \pm 0.6$	$62.7 \pm 0.5$	$64.1 \pm 1.1$
P( <i>n</i> -BA- <i>co</i> -MMA) 2:1	$55.6 \pm 1.1$	$54.6 \pm 0.7$	$56.3 \pm 0.6$
P( <i>n</i> -BA- <i>co</i> -MMA) 3:2	$54.9 \pm 1.5$	$63.3 \pm 2.2$	$53.4 \pm 1.5$

**Table D.3** Surface tension of encapsulated chitosan copolymers with different molecular weights (1%w/v)

Polymer	surface tension (mN/m)		
	1% w/v		
	$1.2 \times 10^5$ Da	$3.7 \times 10^5$ Da	$8.5 \times 10^5$ Da
P( <i>n</i> -BA- <i>co</i> -MMA) 1:1	$64.7 \pm 1.1$	$63.6 \pm 0.7$	$62.6 \pm 0.3$
P( <i>n</i> -BA- <i>co</i> -MMA) 1:2	$63.7 \pm 1.1$	$62.6 \pm 0.6$	$65.3 \pm 0.5$
P( <i>n</i> -BA- <i>co</i> -MMA) 2:1	$58.1 \pm 1.2$	$56.3 \pm 0.9$	$54.1 \pm 0.2$
P( <i>n</i> -BA- <i>co</i> -MMA) 3:2	$58.7 \pm 0.8$	$56.8 \pm 0.9$	$55.4 \pm 0.6$

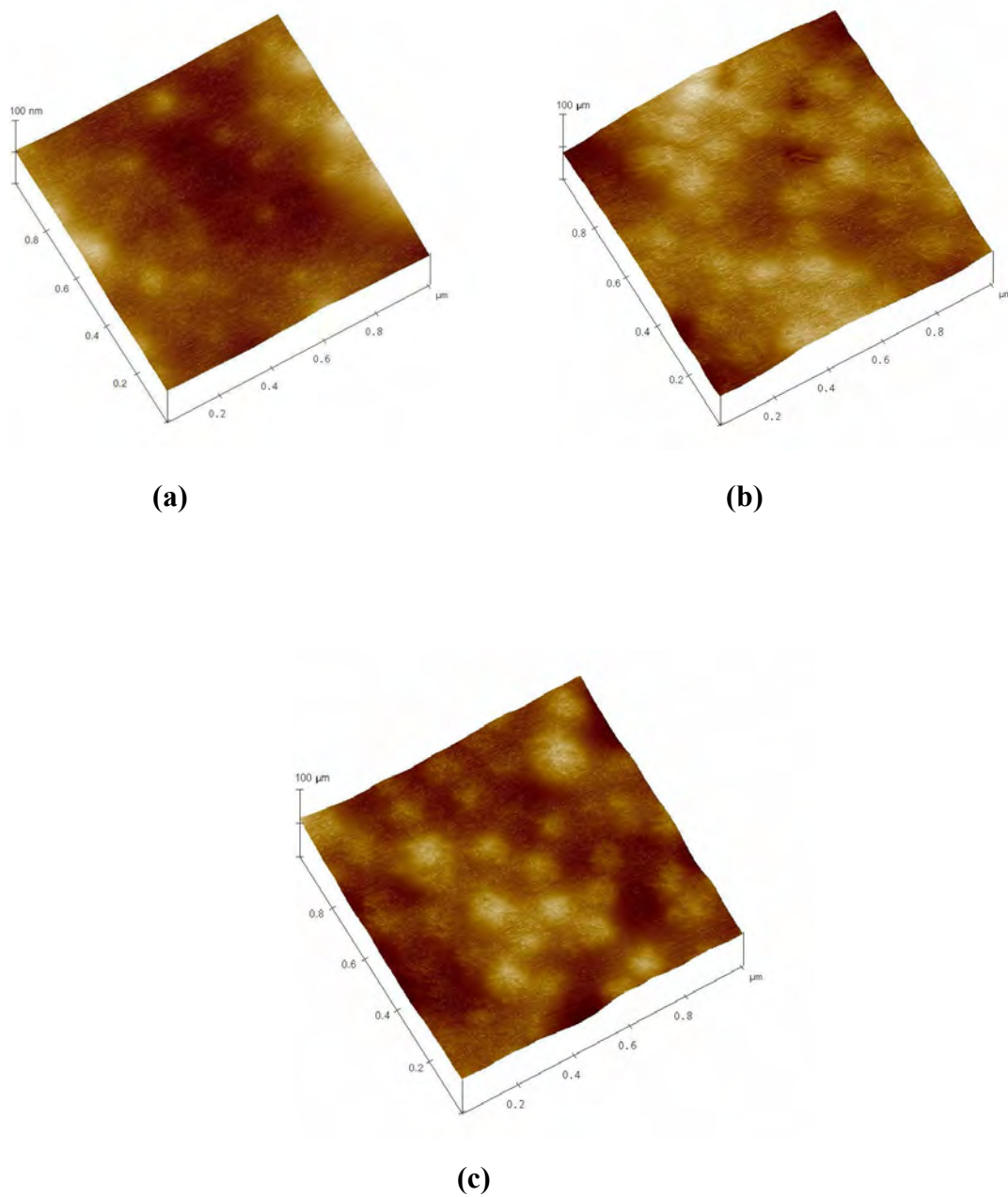
**Table D.4** Surface tension of encapsulated chitosan copolymers with different molecular weights (1.5%w/v)

Polymer	surface tension (mN/m)		
	1.5% w/v		
	$1.2 \times 10^5$ Da	$3.7 \times 10^5$ Da	$8.5 \times 10^5$ Da
P( <i>n</i> -BA- <i>co</i> -MMA) 1:1	$63.1 \pm 0.3$	$63.4 \pm 0.3$	$65.3 \pm 1.5$
P( <i>n</i> -BA- <i>co</i> -MMA) 1:2	$63.9 \pm 0.6$	$60.9 \pm 1.7$	$65.1 \pm 2.0$
P( <i>n</i> -BA- <i>co</i> -MMA) 2:1	$56.6 \pm 1.4$	$56.8 \pm 0.9$	$55.8 \pm 0.2$
P( <i>n</i> -BA- <i>co</i> -MMA) 3:2	$57.8 \pm 1.8$	$62.6 \pm 0.5$	$60.7 \pm 1.2$

**APPENDIX E**  
**EFFECT OF INITIATOR**

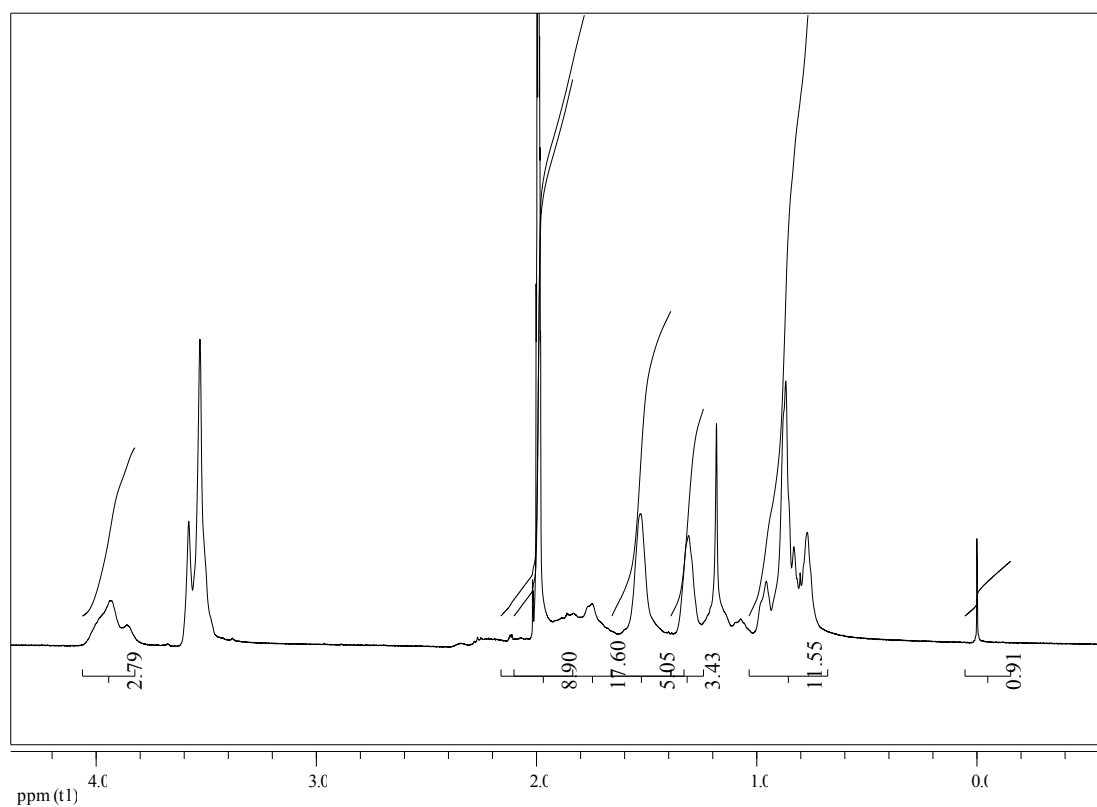
**Table E.1** Particle size and zeta potential of copolymers at 1:1 monomer ratio encapsulated with chitosan (1.5%w/v) with different initiator concentrations

P( <i>n</i> -BA- <i>co</i> -MMA) 1:1	KPS concentration (%w/v)		
	0.1	0.2	0.3
Particle size (nm)	558.0 ± 20.6	462.6 ± 25.5	216.3 ± 6.7
Zeta potential (mV)	45.6 ± 0.5	37.6 ± 0.9	30.4 ± 0.4



**Figure E.1** : AFM images of P(*n*-BA-*co*-MMA) at 1:1 monomer ratio encapsulated with chitosan (1.5% w/v, MW  $3.7 \times 10^5$  Da) with different initiator concentrations (a) 0.1%w/v, (b) 0.2%w/v, (c) 0.3%w/v.

## APPENDIX F

<sup>1</sup>H-NMR RESULT

**Figure F.1 :** <sup>1</sup>H-NMR spectrum of P(*n*-BA-*co*-MMA) at 1:1 monomer ratio encapsulated with chitosan (0.5%w/v, MW  $3.7 \times 10^5$  Da).

$$\text{Total peak area} = \text{Peak area of } n - \text{BA} + \text{Peak area chitosan}$$

$$\% \text{Grafting} = \frac{\text{Peak area of chitosan grafting with } n - \text{BA}}{\text{Total peak area}} \times 100$$

$$\begin{aligned}
 \text{Total peak area} &= 22.82 + 9.81 \\
 &= 32.63 \\
 \%Grafting &= \frac{17.6}{32.63} \times 100 \\
 &= 53.9\%
 \end{aligned}$$

**Table F.1** Grafting percentage of copolymer (1:1) encapsulated with 0.5% w/v of various molecular weights of chitosan (from peak area of  $^1\text{H-NMR}$  spectrum)

Polymer	%Grafting
P( <i>n</i> -BA- <i>co</i> -MMA) 1:1/0.5% (MW $1.2 \times 10^5$ Da)	54.3
P( <i>n</i> -BA- <i>co</i> -MMA) 1:1/0.5% (MW $3.7 \times 10^5$ Da)	53.9
P( <i>n</i> -BA- <i>co</i> -MMA) 1:1/0.5% (MW $8.5 \times 10^5$ Da)	58.6

**Table F.2** Grafting percentage of copolymer (1:1) encapsulated with various chitosan concentrations (from peak area of  $^1\text{H-NMR}$  spectrum)

Polymer	%Grafting
P( <i>n</i> -BA- <i>co</i> -MMA) 1:1/0.5% (MW $3.7 \times 10^5$ Da)	53.9
P( <i>n</i> -BA- <i>co</i> -MMA) 1:1/1% (MW $3.7 \times 10^5$ Da)	67.9
P( <i>n</i> -BA- <i>co</i> -MMA) 1:1/1.5% (MW $3.7 \times 10^5$ Da)	74.8

**Table F.3** Grafting percentage of encapsulated copolymers prepared with various monomer ratios (from peak area of  $^1\text{H-NMR}$  spectrum)

Polymer	%Grafting
P( <i>n</i> -BA- <i>co</i> -MMA) 1:2/0.5% (MW $3.7 \times 10^5$ Da)	28.0
P( <i>n</i> -BA- <i>co</i> -MMA) 1:1/0.5% (MW $3.7 \times 10^5$ Da)	53.9
P( <i>n</i> -BA- <i>co</i> -MMA) 3:2/0.5% (MW $3.7 \times 10^5$ Da)	58.2
P( <i>n</i> -BA- <i>co</i> -MMA) 2:1/0.5% (MW $3.7 \times 10^5$ Da)	59.5

## VITA

Miss Wikanda Taweerat was born on January 18, 1983 in Chonburi. She graduated with a Bachelor's degree of Science in Chemistry from Burapha University in 2005. She graduated with a Master's Degree in Petrochemistry and Polymer Science, Graduate School, Chulalongkorn University, in 2008.